International Journal of Mass Spectrometry 349–350 (2013) 203–218

Contents lists available at ScienceDirect

International Journal of Mass Spectrometry

journal homepage: www.elsevier.com/locate/ijms

Applications of accelerator mass spectrometry

Walter Kutschera*

Vienna Environmental Research Accelerator (VERA), Faculty of Physics, University of Vienna, 1090 Vienna, Austria

ARTICLE INFO

Article history:
Received 14 May 2013
Accepted 20 May 2013
Available online 6 June 2013

Keywords:
Accelerator mass spectrometry
Long-lived radionuclides
Applications
Environmental science

ABSTRACT

Applications of accelerator mass spectrometry (AMS) evolved into multi-disciplinary research covering virtually every domain of our environment at large. The possibilities of applications are clearly coupled to technical developments of AMS, which will be covered by the accompanying article of H.-A. Synal. The present review therefore concentrates on describing AMS applications to the largest extent possible. Since the knowledge of the author on the many fields where AMS measurements are performed is, of course, limited, the selection of examples discussed in this review is somewhat biased. In order to compensate for this, a rather long list of references is presented, which should be consulted for a deeper understanding of the respective fields. The seven domains of our environment at large (atmosphere, biosphere, hydrosphere, cryosphere, lithosphere, cosmosphere, and technosphere) are being used as a guideline for the present review.

1. Introduction

Accelerator mass spectrometry (AMS) is arguably the most sensitive method to measure long-lived radionuclides with isotopic abundances as low as 10^{-12} to 10^{-16}. It should be noted at the onset that the term ‘long-lived’ has a different meaning in geochronology [1], where long-lived radionuclides are the ones which survive the age of the solar system (e.g. ^{232}Th, ^{238}U), and radionuclides measured with AMS (e.g. ^{14}C, ^{10}Be) are called short-lived. In general, radionuclides can be detected through the radiation emitted in their decay or directly by atom counting with mass spectrometry. The method of choice depends on a variety of factors [2]. As in most analytical methods, background limits the ultimate sensitivity. For decay counting it is primarily secondary radiation from cosmic rays or environmental radioactivity, whereas in mass spectrometry it is interference from isobaric atoms or molecules. If the half-life is in the order of the observation time, decay counting is still the most sensitive detection method. For example, in the famous Homestake solar neutrino experiment [3], the decay of about 20 atoms of ^{37}Ar ($t_{1/2} = 35$ d) are counted underground in miniature gas-filled proportional counters. Since they were produced in 615 tons of perchlorethylene liquid (C_2Cl_4), a detection sensitivity of approximately 10^{-29} was achieved.

When the half-life is much longer than the observation time, the direct counting of atoms by mass spectrometry becomes superior. For example, less than one millionth of the ^{14}C atoms in a sample decay in one day ($t_{1/2} = 5700$ year), while counting ^{14}C atoms directly by mass spectrometry can be orders of magnitudes more sensitive [4]. However, efforts to measure the extremely low isotopic abundance of ^{14}C ($^{14}C/^{12}C = 1.2 \times 10^{-12}$) by regular mass spectrometry fell short by about one order of magnitude [5]. The break-through came in 1977, when several nuclear physics laboratories realized that the use of an entire accelerator system as a mass spectrometer provided the necessary discrimination against background. First experiments were performed at a cyclotron [6] and at tandem accelerators [7–9].

Historically it is interesting to note that the use of accelerators as mass spectrometers started much earlier. In 1939, Louis Alvarez used the 60-inch cyclotron at Berkeley to detect ^{3}He in helium [10], and subsequently showed that tritium (^{3}H) is radioactive [11] by bombarding deuterium with deuterons. This was an important discovery because it showed that ^{3}He and not tritium was the stable mass-3 nuclide, contrary to what was believed at that time [12]. Many years later, Alvarez described these early days of mass spectrometry in a reminiscent article in Physics Today [13].

When AMS was revived in 1977, tandem accelerators quickly turned out to be ideal for the detection of ^{14}C because carbon forms prolific negative ions, and negative ions of ^{14}N are unstable [7]. In addition, interferences from mass-14 molecules, e.g. $^{12}CH_2^-$ and $^{13}CH^-$, are efficiently removed by dissociating the molecules in the stripping process of the tandem accelerator. In the ensuing years, AMS was quickly extended to other long-lived radionuclides (e.g. ^{10}Be, ^{26}Al, ^{36}Cl, ^{41}Ca, ^{129}I). One of them (^{41}Ca), although suggested as an interesting dating tool some time ago [14,15], had never been detected at natural concentrations by decay counting. Eventually, AMS made it possible [16], and some interesting applications emerged [17].

---

* Corresponding author. Tel.: +43 1427751759; fax: +43 142779517.
E-mail address: walter.kutschera@univie.ac.at

1387-3806/$ – see front matter © 2013 Elsevier B.V. All rights reserved.
http://dx.doi.org/10.1016/j.ijms.2013.05.023

Fig. 1. Distribution of AMS facilities around the world, with approximately 100 active facilities (Courtesy of Christof Vockenhuber).

During the past 30 years, a number of reviews covering both methodology and applications of AMS were published [18–31]. In addition, one text book on AMS is available [32]. Starting in 1978 at the University of Rochester, the tri-annual AMS conferences cover detailed developments in the field. The 12th AMS conference took place 2011 in Wellington, New Zealand. References to all previous conferences can be found in the proceedings of this conference [33]. The current review will concentrate primarily on the large range of application of AMS, whereas the accompanying review by Synal [34] will cover AMS methodology, particularly the development of ever smaller AMS facilities.

Almost all AMS facilities in the world are based on tandem accelerators, because, on the one hand, they are ideally suited for ^{14}C measurements for the reasons mentioned above, and, on the other hand, almost all elements form stable negative ions and can be readily produced in cesium-beam sputter sources [35,36]. The exception are Be, N, Mg, Ar, Mn, Kr, Zn, Xe, Hg, but for some radionuclides within this group negative molecules are being used (^{10}BeO^{-}, ^{53}MnO^{-}). Currently, there are about 100 AMS facilities in the world (Fig. 1), with approximately half of them considered to be small (terminal voltage 0.2–1.0 MV), one quarter to be medium-size (3 MV), and one quarter to be large (5–10 MV). Also, a few very large tandem accelerators (14–25 MV) are used for AMS.

Since noble gases do not form stable negative ions, AMS of ^{39}Ar and ^{81}Kr require positive-ion accelerators [26,37]. Recently, a radionuclide of geochronological importance (^{146}Sm) has also been investigated with positive ions [38]. In all cases multiply charged positive ions were produced in an ECR (electron cyclotron resonance) source, and accelerated to high energy either in a cyclotron or a linear accelerator. At these higher energies, a gas-filled magnetic spectrograph can be used as a powerful tool for isobar separation [39]. The much lower energy of small and medium-size tandem accelerators limits the use of some interesting radionuclides because of incomplete isobar separation. Efforts are under way to improve this situation: (i) Selective removal of isobaric interferences by interaction of lasers with negative ions [40,41], (ii) Selective negative-ion chemistry in reaction cells [42,43]. This may eventually allow one to utilize most of the long-lived radionuclides throughout the nuclear chart. A recent boost to the efficiency of detecting heavy radioisotopes with smaller tandem accelerators is the introduction of helium as stripper gas [44].

2. Radionuclides used with AMS

Table 1 lists 55 radionuclides which have been used so far in AMS experiments. With a few exceptions their half-lives is longer than 100 years, and comprise approximately half of the radionuclides which exist in this time range in nature. Originally, only 5 radionuclides (^{10}Be, ^{14}C, ^{26}Al, ^{36}Cl, ^{129}I) were pursued with AMS

Table 1
Radionuclides measured with AMS.

Radionuclide	Half-life (year)	Reference
^{3}H	$(1.2320 \pm 0.0022) \times 10^{1}$	[45]
^{10}Be	$(1.387 \pm 0.012) \times 10^{6}$	[46]
^{14}C	$(5.700 \pm 0.030) \times 10^{3}$	This compilation
^{26}Al	$(7.18 \pm 0.18) \times 10^{5}$	This compilation
^{32}Si	$(1.44 \pm 0.11) \times 10^{2}$	[47]
^{36}Cl	$(3.013 \pm 0.015) \times 10^{5}$	[48]
^{39}Ar	$(2.69 \pm 0.03) \times 10^{2}$	[49]
^{40}K	$(1.248 \pm 0.003) \times 10^{9}$	[50]
^{41}Ca	$(9.94 \pm 0.15) \times 10^{4}$	[51]
^{44}Ti	$(5.89 \pm 0.03) \times 10^{1}$	[52]
^{53}Mn	$(3.7 \pm 0.4) \times 10^{6}$	[53]
^{55}Fe	$(2.744 \pm 0.009) \times 10^{0}$	[54]
^{59}Ni	$(7.6 \pm 0.5) \times 10^{4}$	[55]
^{60}Fe	$(2.62 \pm 0.04) \times 10^{6}$	[56]
^{63}Ni	$(1.001 \pm 0.020) \times 10^{2}$	[57]
^{68}Ge	$(7.418 \pm 0.005) \times 10^{-1}$	[58]
^{79}Se	$(3.77 \pm 0.19) \times 10^{5}$	[59]
^{81}Kr	$(2.29 \pm 0.11) \times 10^{5}$	[60]
^{90}Sr	$(2.879 \pm 0.006) \times 10^{1}$	[61]
^{93}Zr	$(1.61 \pm 0.05) \times 10^{6}$	[62]
^{99}Tc	$(2.111 \pm 0.012) \times 10^{5}$	[63]
^{126}Sn	$(2.17 \pm 0.14) \times 10^{5}$	This compilation
^{129}I	$1.57 \pm 0.04) \times 10^{7}$	[64]
^{135}Cs	$(2.3 \pm 0.3) \times 10^{6}$	[65]
^{137}Cs	$(3.008 \pm 0.009) \times 10^{1}$	[66]
^{146}Sm	$(6.8 \pm 0.7) \times 10^{7}$	[38]
^{151}Sm	$(9.0 \pm 0.8) \times 10^{1}$	[67]
^{182}Hf	$(8.90 \pm 0.09) \times 10^{6}$	[68]
^{202}Pb	$(5.25 \pm 0.28) \times 10^{4}$	[69]
^{205}Pb	$(1.73 \pm 0.07) \times 10^{7}$	[70]
^{210m}Bi	$(3.04 \pm 0.06) \times 10^{6}$	[71]
^{228}Th	$(1.9116 \pm 0.0016) \times 10^{0}$	[72]
^{229}Th	$(7.880 \pm 0.120) \times 10^{3}$	[73]
^{230}Th	$(7.54 \pm 0.03) \times 10^{4}$	[74]
^{231}Pa	$(3.276 \pm 0.011) \times 10^{4}$	[75]
^{232}Th	$(1.40 \pm 0.01) \times 10^{10}$	[76]
^{232}U	$(6.89 \pm 0.04) \times 10^{2}$	[77]
^{233}U	$(1.592 \pm 0.002) \times 10^{5}$	[78]
^{234}U	$(2.455 \pm 0.006) \times 10^{5}$	[79]
^{235}U	$(7.04 \pm 0.01) \times 10^{8}$	[79]
^{236}U	$(2.342 \pm 0.004) \times 10^{7}$	[79]
^{237}Np	$(2.144 \pm 0.007) \times 10^{6}$	[80]
^{238}U	$(4.468 \pm 0.003) \times 10^{9}$	[81]
^{239}Pu	$(2.4110 \pm 0.0030) \times 10^{4}$	[82]
^{240}Pu	$(6.561 \pm 0.007) \times 10^{3}$	[83]
^{241}Pu	$(1.4290 \pm 0.0006) \times 10^{1}$	[84]
^{241}Am	$(4.326 \pm 0.006) \times 10^{2}$	[84]
^{242}Pu	$(3.75 \pm 0.02) \times 10^{5}$	[79]
^{243}Am	$(7.370 \pm 0.040) \times 10^{3}$	[85]
^{244}Pu	$(8.00 \pm 0.09) \times 10^{7}$	[79]
^{244}Cm	$(1.81 \pm 0.01) \times 10^{1}$	[79]
^{246}Cm	$(4.760 \pm 0.040) \times 10^{3}$	[79]
^{247}Cm	$(1.56 \pm 0.05) \times 10^{7}$	[79]
^{248}Cm	$(3.48 \pm 0.06) \times 10^{5}$	[79]
^{250}Cm	$(\sim 8.3) \times 10^{3}$	[86]

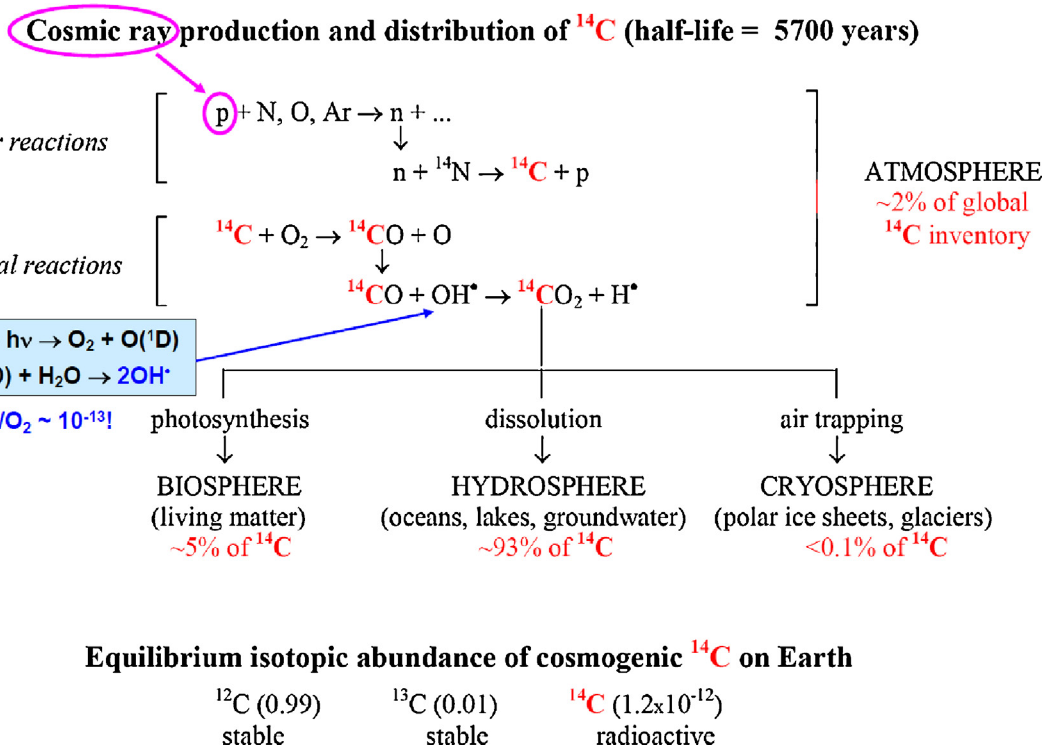

Fig. 2. Schematic presentation of the processes leading to the production and distribution of ^{14}C on Earth [104]. The fraction of the global ^{14}C inventory for the different archives is given in percent. The oxidation of carbon to CO$_2$ is a two-step process, where the very reactive OH radical plays an important role [105]. As indicated in the box, the main production path of OH depends on the availability of ozone, light and humidity, and due to its very short residence time in the atmosphere (~1 s) the concentration of OH relative to O$_2$ is extremely small.

[20], but gradually many more became available. An attempt has been made in Table 1 to present the best possible values for the half-lives of the radionuclides, with their respective reference. For some of the radionuclides, AMS measurements were used to obtain better half-lives (see Section 4.7.1). However not always an accurate half-life value is known, because sometimes conflicting measurements for a particular radionuclide exist. Therefore, for any application where the half-life and its uncertainty really matters, the respective reference should be consulted.

There are two important radionuclides for AMS (^{14}C, ^{26}Al), where new compilations are presented in Table 1. For ^{14}C, a half-life value of (5730 ± 40) year [87] was used for many years by the radiocarbon community. The slightly revised value of (5700 ± 30) year was determined from the following four half-life measurements: (5780 ± 65) year [88], (5680 ± 30) year [89], (5745 ± 50) year [90], and (5660 ± 40) year [91]. The new value is the weighted mean of these four measurements, with a ‘scaled uncertainty’ calculated following the procedure of the Particle Data Group [92]. The resulting (rounded) value is consistent with the one reported by the National Nuclear Data Centre of Brookhaven National Laboratory (http://www.nndc.bnl.gov).

For ^{26}Al, the weighted mean of three values from the literature, $(7.16 \pm 0.32) \times 10^5$ year [93], $(7.05 \pm 0.24) \times 10^5$ year [94], and $(7.8 + 0.5) \times 10^5$ year [95] was determined. For the fission product ^{126}Sn, the weighted mean and a scaled uncertainty were determined from five values in the literature [96–101]. The new half-life values of ^{60}Fe and ^{146}Sm listed in Table 1 are in clear contradiction to previous measurements and await confirmation by additional experiments.

3. ^{14}C – a gift from nature

In 1912 Victor Hess discovered cosmic rays with balloon flights around Vienna [102], and 34 years later Willard Libby figured out at the University of Chicago that ^{14}C must be produced by cosmic rays in the atmosphere [103], eventually entering the biosphere and the hydrosphere through the CO$_2$ cycle (Fig. 2).

Biogenic ^{14}C was detected for the first time in methane from a sewage disposal plant in Baltimore [106]. This paper also discusses earlier considerations about cosmic-ray neutrons and their capture in nitrogen. The use of ^{14}C as a dating tool in archeology was established by measuring its content in objects of known age [107]. In 1960, Willard Libby received the Nobel Prize in Chemistry “for his method to use carbon-14 for age determination in archeology, geophysics, and other branches of physics” [108]. At that time ^{14}C was still measured through the beta radiation requiring sample sizes of several grams of carbon. With the advent of AMS sample sizes could be reduced by factors of thousand and more, substantially enlarging the range of applications.

In Table 2 some of the remarkable properties of ^{14}C are summarized. In addition to its unique properties as a dating tool for organic matter in the 50,000-year range, it has atomic properties which makes it ideal for AMS measurements with tandem accelerators. This allowed the development of ever smaller AMS facility described in the accompanying contribution by Synal [34].

4. Applications of AMS

Although ^{14}C measurements dominate applications of AMS, a large variety of other radionuclides were made accessible through AMS (Table 1). AMS applications are being performed in essentially every domain of our environment at large. In order to describe the enormous breadth of these applications, it is convenient to divide the environment into seven large domains [115]: atmosphere, biosphere, hydrosphere, cryosphere, lithosphere, cosmosphere, and technosphere. While the first five domains are natural archives on Earth, the cosmosphere refers to extraterrestrial matter, and

Table 2
The unique properties of ^{14}C.

Property	Comment
Favorable production process	Spallation reactions of cosmic rays in the atmosphere liberate neutrons, which in turn produce ^{14}C through the ^{14}N(n,p)^{14}C reaction. The high nitrogen content of the atmosphere (78% N_2) results in a production rate of ~2 ^{14}C atoms cm^{-2} s^{-1} [109], which is higher than that of other long-lived radionuclides (Fig. 3).
Uniform atmospheric distribution	^{14}C oxidizes to $^{14}CO_2$ (Fig. 1) and becomes part of the well-mixed tropospheric CO_2 content. Since the production of neutrons by cosmic rays in the atmosphere is altitude and latitude dependent [110], atmospheric mixing is important to provide a nearly uniform $^{14}CO_2$ concentration in the troposphere around the globe.
Photosynthesis of plants	Plants take up atmospheric $^{14}CO_2$ through photosynthesis, which is the main path of ^{14}C to enter the biosphere.
High solubility of CO_2	The solubility of CO_2 in water is 0.04 mol/L H_2O at NTP. This is 30 and 60 times higher than that of O_2 and N_2, respectively, and leads to a relatively high $^{14}CO_2$ content of the oceans.
Radiocarbon dating	After death, organic material stops the uptake of ^{14}C and the long half-life ($t_{1/2}$ = 5700 years) is ideally suited as a radioactive clock for the last 50,000 years, covering the decisive period for the development of modern humans.
Strongly hindered beta decay	The beta decay of ^{14}C to ^{14}N (a so called Gamov–Teller transition) is unusually hindered due to nuclear structure effects [111]. A normal transition strength, as it is observed in neighboring nuclides, would lead to a half-life of only about 50 days making it completely useless for archeological dating. The actual half-life is (5700 ± 30) year (Table 1).
No build-up of ^{14}C after death	Due to the low isotopic abundance of ^{13}C (1.1%), and the small cross section for the ^{13}C(n,γ)^{14}C reaction (σ = 1.4 mbarn), ^{14}C build-up by environmental neutrons in organic matter after death is negligible.
Calibration of ^{14}C	The determination of an absolute age with ^{14}C requires to know the atmospheric ^{14}C content as a function of time. This has been established by ^{14}C measurements in objects of known age such as tree rings, corals, stalagmites [112]. Recently the calibration beyond the range of tree rings (~12,000 years) has been improved with varved lake sediments [113].
Mass fractionation correction	Because carbon has two stable isotopes, mass fractionation both in natural and in instrumental processes can be determined through ^{13}C/^{12}C ratio measurements, and the effect on ^{14}C can be corrected correspondingly [114].
The ideal AMS nuclide	Negative ion currents of around 50 μA $^{12}C^-$ can easily be produced from solid graphite in a cesium-beam sputter source. With a modern ^{14}C/^{12}C ratio of 1.2×10^{-12}, about 400 $^{14}C^-$ ions per second are then emitted from a carbon sample of 1 mg, and half of it ends up in the final particle detector. Even for a 50,000-year old sample, one will still detect about 12 ^{14}C atoms per minute. Most important is the suppression of the stable isobar ^{14}N in the ion source due to the instability of N^- [7].

the technosphere refers to the domain where man-made radionuclides matter. An updated version of these seven domains with their respective fields of AMS application and radioisotopes is shown in Table 3. In the following the AMS applications will be discussed according to these seven domains. However, these divisions are merely guidelines since often the interactions between the domains are investigated with the help of radionuclides measured with AMS.

Since it is virtually impossible to describe the very large number of applications of AMS in this review, only a representative selections can be discussed. It is hoped, though, that this will still convey the flavor of the versatility of AMS as an analytic tool to study our environment at large.

4.1. Atmosphere

The atmosphere is the main source for radionuclides produced by cosmic-ray interaction [116]. Fig. 3 shows the production rate of long-lived radionuclides used in AMS [37].

Since one assumes that cosmic-ray bombardment persisted much longer than the respective half-lives, secular equilibrium between production and decay has been reached on Earth. The differential equation which describes production and decay of a radionuclide is:

$$\frac{dN}{dt} = -\lambda N + P \qquad (1)$$

where N denotes the number of radionuclides, and P the production rate, λ is the decay constant, which is related to the mean lifetime, τ, and the half-life, $t_{1/2}$, through the relation $\lambda = 1/\tau = \ln 2/t_{1/2}$. When secular equilibrium is reached, then $dN/dt = 0$, and therefore $N = P/\lambda = P\tau = (P/\ln 2)t_{1/2}$. This means that the maximum number of atoms for a radionuclide on Earth is equal to the production rate times its mean lifetime. In cases where the atmosphere is the main

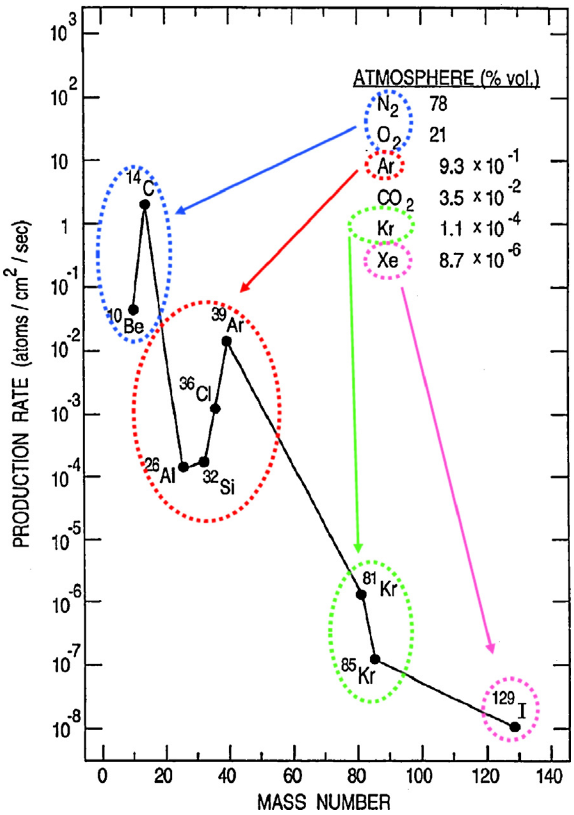

Fig. 3. Cosmogenic production rates of long-lived radioisotopes in the atmosphere [37]. The production rate is dominated by the availability of suitable target atoms in the atmosphere, indicated by the composition of the atmosphere, and the respective radionuclides connected to it. The total production rate on Earth (atoms/s) can be obtained by multiplying with the surface of the Earth (5.1×10^{18} cm^2).

Table 3
Overview of research areas where AMS measurements are used.

Domain/research area	Radionuclide[a]
Atmosphere	
Production of radionuclides by cosmic-ray interaction	$^{10}\mathrm{Be}$, $^{14}\mathrm{C}$, $^{26}\mathrm{Al}$, $^{32}\mathrm{Si}$, $^{36}\mathrm{Cl}$, $^{39}\mathrm{Ar}$, $^{81}\mathrm{Kr}$, $^{129}\mathrm{I}$
Chemistry and dynamics of CO, CO_2, CH_4	$^{14}\mathrm{C}$, ^{14}C
Mixing of stratospheric and tropospheric air	^{14}C, $^{10}\mathrm{Be}$
Releases from nuclear industry	^{14}C, ^{99}Tc ^{129}I
Fossil fuel effect, 'dead' CO_2	^{14}C
Bomb peak from nuclear weapons testing	^{14}C
Biosphere	
Radiocarbon dating in archeology and other fields	$^{14}\mathrm{C}$
$^{14}\mathrm{C}$ calibration (tree rings, corals, sediments, speleothems)	$^{14}\mathrm{C}$
Development of radiocalcium dating of bones	$^{41}\mathrm{Ca}$
Bomb-peak dating (forensic medicine, dating DNA)	^{14}C
Microdosing for drug development	^{14}C
In vivo tracer studies in plants, animals, humans	^{14}C, ^{26}Al, ^{41}Ca
Hydrosphere	
Dating of groundwater (important freshwater source)	$^{14}\mathrm{C}$, [$^{39}\mathrm{Ar}$], $^{36}\mathrm{Cl}$, $^{81}\mathrm{Kr}$, $^{129}\mathrm{I}$
Global ocean currents	$^{14}\mathrm{C}$, ^{14}C, $^{39}\mathrm{Ar}$, ^{99}Tc, ^{129}I, $^{231}\mathrm{Pa}$, ^{236}U
Paleoclimatic studies in lake and ocean sediments	$^{14}\mathrm{C}$
Cryosphere	
Paleoclimate studies in polar ice sheets	$^{10}\mathrm{Be}$, $^{14}\mathrm{C}$, $^{26}\mathrm{Al}$, $^{36}\mathrm{Cl}$, [$^{81}\mathrm{Kr}$]
Paleoclimate studies in glaciers	$^{14}\mathrm{C}$, $^{32}\mathrm{Si}$
Tracing solar variability in time (Greenland ice cores)	$^{10}\mathrm{Be}$, $^{14}\mathrm{C}$, $^{36}\mathrm{Cl}$
Bomb-peak record in recent ice	^{36}Cl, ^{41}Ca, ^{129}I
Lithosphere	
Exposure dating of rocks (deglaciation, geomorphology, erosion)	$^{10}\mathrm{Be}$, $^{14}\mathrm{C}$, $^{26}\mathrm{Al}$, $^{36}\mathrm{Cl}$, $^{53}\mathrm{Mn}$
Paleoclimatic studies in loess	$^{10}\mathrm{Be}$, $^{14}\mathrm{C}$
Tectonic plate subduction studies	$^{10}\mathrm{Be}$
Neutron flux monitor in uranium minerals	$^{236}\mathrm{U}$
Cosmosphere	
Cosmogenic nuclides in meteorites and lunar material	$^{10}\mathrm{Be}$, $^{14}\mathrm{C}$, $^{26}\mathrm{Al}$, $^{36}\mathrm{Cl}$, $^{41}\mathrm{Ca}$, $^{53}\mathrm{Mn}$, $^{59}\mathrm{Ni}$, $^{60}\mathrm{Fe}$
Live supernovae remnants in terrestrial materials	$^{26}\mathrm{Al}$, $^{60}\mathrm{Fe}$, $^{244}\mathrm{Pu}$ [$^{146}\mathrm{Sm}$, $^{182}\mathrm{Hf}$, $^{247}\mathrm{Cm}$],
Stable trace isotopes in presolar grains	$^{194,195,196,198}\mathrm{Pt}$
Geochemical solar neutrino detection	[$^{97,98}\mathrm{Tc}$, $^{205}\mathrm{Pb}$]
Search for superheavy elements in terrestrial materials	Eka-Th, Ds, Rg, Fl, Eka-Bi ($A \sim 300$, $Z \sim 114$)
Search for exotic particles in Nature	Free quarks, very heavy isotopes, strange matter
Technosphere	
Half-life measurements—Depth profiling in fusion walls	^{32}Si, $^{41}\mathrm{Ca}$, ^{44}Ti, ^{60}Fe, ^{79}Se, ^{126}Sn, ^{146}Sm, ^{3}H
Possible fusion plasma thermometer	$^{27}\mathrm{Al(n,2n)}^{26}Al$
Reaction studies for nuclear astrophysics	^{10}Be, ^{14}C, ^{26}Al, ^{36}Cl, ^{41}Ca, ^{44}Ti, ^{55}Fe, ^{59}Ni, ^{63}Ni, ^{68}Ge, ^{146}Sm, ^{202}Pb, $^{209\mathrm{m}}Bi$, ^{230}Th, ^{231}Pa
Neutron dosimetry of the Hiroshima bomb	^{36}Cl, ^{41}Ca, ^{63}Ni
Nuclear safeguards	$^{146,\ 149,\ 151}Sm$, ^{233}U, ^{236}U, ^{237}Np, $^{239,240,241,242,244}Pu$

[a] Radionuclides measured with AMS in the respective area of application. Italicized radionuclides are man-made. Radionuclides in square brackets indicate their potential use in the corresponding research area, but AMS detection at the required sensitivity level has not yet been fully developed. For the respective half-lives see Table 1.

archive for a radionuclide (e.g. for ^{39}Ar and ^{81}Kr), this number can be obtained by measuring either its activity concentration or its isotope ratio in air. Combining the respective half-lives from Table 2 with the corresponding production rates and atmospheric abundances of Ar and Kr from Fig. 3, one obtains isotope ratios which are close to the observed ones: $^{39}\mathrm{Ar/Ar} = 8.1 \times 10^{-16}$ [117], and $^{81}\mathrm{Kr/Kr} = 5.2 \times 10^{-13}$ [118]. When the distribution on Earth is more complex as in the case of ^{14}C, the total inventory is distributed between different archives (see Fig. 2).

4.1.1. *Measurements of $^{14}CO_2$, ^{14}CO, $^{14}CH_4$*

Measurements of ^{14}C in atmospheric CO_2 started well before the advent of the AMS technique [119], and to this day can be performed by beta counting if large air samples (~10,000 L) are available. These measurements already revealed a clear picture of the ^{14}C excess produced by the atmospheric nuclear weapons testing period between 1950 and 1963 [119]. However, often there is much less material available, and AMS measurements of high accuracy have been developed for air samples of a few liters [120].

In order to measure the ^{14}C production directly in air at higher altitudes, compressed-air cylinders were carried along cruising altitudes of commercial airplanes for two years, and the resulting $^{14}CO_2$ and ^{14}CO contents were measured with AMS [121]. The comparison with model calculation showed significant deviation from both the production rate and the $^{14}CO_2/^{14}CO$ ratio. More of these direct measurements would be useful particularly for ^{14}CO, since it is used as a proxy to monitor the hydroxyl radical (OH) concentration in air [122–124]. OH has been called the "detergent" of the atmosphere [105], because of its oxidizing power and its important role to remove trace gases [125].

Another trace gas of considerable importance in the ongoing debate about global warming is methane (CH_4). Although its concentration in the atmosphere is about a factor of 200 lower than the one of CO_2, the global warming potential of CH_4 is 25 times higher on a molecule-to-molecule comparison [126]. At present, the radiative forcing (expressed in W/m^2) of CH_4 is about a factor of four smaller than the one of CO_2 [127]. $^{14}CH_4$ has been studied with AMS in the atmosphere, e.g. [128–130], and recently also in CH_4

extracted form Greenland ice around the last glacial termination [131].

4.1.2. ^{10}Be/^{7}Be ratio measurements to study stratosphere-to-troposphere transport

Within the EU project STACCATO (Influence of Stratosphere–Troposphere Exchange in A Changing Climate on Atmospheric Transport and Oxidation Capacity), particle-bound beryllium isotopes were investigated in air filters and the ratio between long-lived ^{10}Be ($t_{1/2} = 1.39 \times 10^6$ year) measured with AMS, and short-lived ^{7}Be (53.3 d) measured with gamma spectrometry, was evaluated [132]. Since there is a considerable difference of the residence time of Be in the stratosphere (about one year) and the troposphere (about three weeks), the different ^{10}Be/^{7}Be ratios can be used as fingerprints of the respective air masses.

4.1.3. ^{26}Al/^{10}Be ratios in the atmosphere and surface firn

The production rate of ^{26}Al in the air is about 500 times smaller than the one of ^{10}Be (cf. Fig. 3), reflected also in the atom ratio of these radionuclides measured in air filters and surface firn at different locations on Earth [133]. Since the mean value of ^{26}Al/^{10}Be $= 1.89 \times 10^{-3}$ was found to be globally constant within 5%, there is hope to use this ratio as a chronometer to date old ice [133]. It is interesting to note that the in situ production of ^{10}Be and ^{26}Al in quartz results in a ^{26}Al/^{10}Be ratio of ~6 (see Sections 4.5.1. and 4.5.3.), which is a factor of ~3000 larger than the meteoric ratio of the atmosphere mentioned above.

4.2. Biosphere

The most important radionuclide in the biosphere is ^{14}C (cf. Fig. 1). Numerous applications arise from this fact, and the dedicated journal Radiocarbon (http://www.radiocarbon.com) records many of these investigations since 1959. Here, only a few typical measurements will be reported.

4.2.1. Radiocarbon dating in archeology

The half-life of ^{14}C is ideally suited to investigate the development of modern humans since the last 50,000 years, and particularly since the dawn of civilization in the Near East about 10,000 years ago. For the latter part a reliable ^{14}C calibration was established by dendrochronology [112], and a recent extension now reaches back to the full time range of ^{14}C dating [113]. For the last 4500 years ^{14}C dating has been found to be in reasonable overall agreement with the historical chronology of ancient Egypt [134]. There are, however, persistent discrepancies of about 100 years between ^{14}C and archeological dating in the second millennium BC for the excavation in Tell el-Daba in the Nile Delta [135], and for the volcanic eruption of Santorini [136,137]. In general, ^{14}C dating in archeology starts with sample taking in the field, and great strides are made nowadays to meticulously follow the entire process from the field through the sample preparation to the final AMS measurement [138].

An interesting field of research in archeology (and in anthropology) is the appearance of anatomically modern man in Central Europe some 40,000 years ago, and its relation to the Neanderthal, e.g. [139–141]. This usually involves dating collagen in bone, which sometimes is degraded to a level which does not allow reliable dating results. An interesting example has recently been reported, which pushes the demise of the Neanderthal further back in time [142].

4.2.2. Dating human DNA with the ^{14}C bomb peak

A few years ago, an exciting possibility to determine retrospectively the birth of cells in humans was developed at the Karolinska Institute in Stockholm [143].

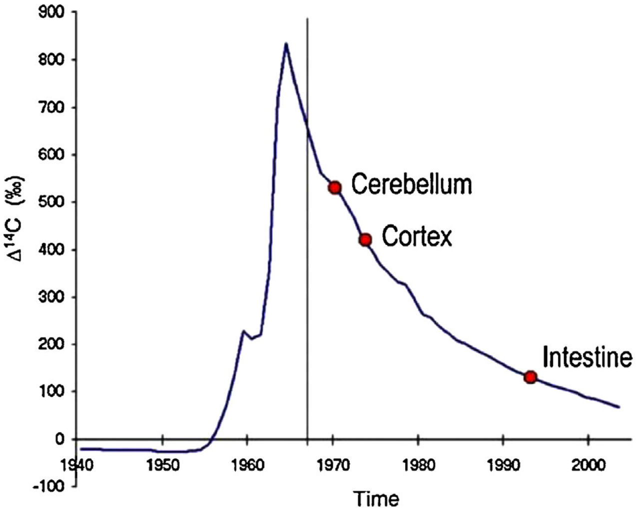

Fig. 4. ^{14}C excess of atmospheric CO$_2$ due to above-ground nuclear weapons testing – which stopped in 1963 – for the second half of the 20th century [144]. The Δ^{14}Cvalues below zero before 1955 are due to the 'dead' CO$_2$ contribution from burning fossil fuel. The vertical line indicates the birth date of an individual. The ^{14}C level of the DNA extracted from cells of different parts of the body (filled circles) indicate that new cells are formed at different times after birth [143].

The above-ground nuclear weapons testing between 1950 and 1963 doubled the ^{14}C content of the atmosphere, which after the nuclear test ban in 1963 dropped back to almost normal in the ensuing 50 years [144]. This rapidly varying ^{14}C excess effectively labeled every living species on Earth including humans. The basic principle to deduce the birth date of cells in humans is quoted here from Spalding et al. [143]: "Most molecules in a cell are in constant flux, with the unique exception of genomic DNA, which is not exchanged after a cell has gone through its last division. The level of ^{14}C integrated into genomic DNA should thus reflect the level in the atmosphere at any given point, and we hypothesized that determination of ^{14}C levels in genomic DNA could be used to retrospectively establish the birth date of cells in the human body." Fig. 4 reproduced from this seminal work demonstrates the method.

In a collaboration between the VERA lab in Vienna and the Karolinska Institute in Stockholm the olfactory bulb system in humans was investigated [145]. Here only a few microgram of DNA were available for the ^{14}C AMS measurements, demanding a particular careful sample preparation in every step from the human tissue to the final carbon sample [146]. It was found that very little if any new neurons were formed in the human olfactory bulb after birth [145], in stark contrast to rodents where 50% turnover in adulthood has been observed.

4.2.3. Biomedical experiments with ^{26}Al and ^{41}Ca

Since natural ^{26}Al/^{27}Al and ^{41}Ca/^{40}Ca isotope ratios are exceedingly small in humans, in the range of 10^{-14}, and the half-lives are much longer than the one of ^{14}C (Table 1), strong radionuclide signals can be administered to humans. Pioneering long-time experiments in humans have been performed for ^{26}Al [147] and ^{41}Ca [148], following the radionuclide concentrations over 5–4 orders of magnitude, respectively. Although some interesting implication for studies of osteoporosis were indicated in a ^{41}Ca labeling experiment by Freeman et al. [149], followed up by another extensive study of Denk et al. [150], ^{41}Ca has not yet entered the realm of drug developments. Also ^{26}Al has not yet entered this stage, e.g. for kidney related problems where Al may play an important role.

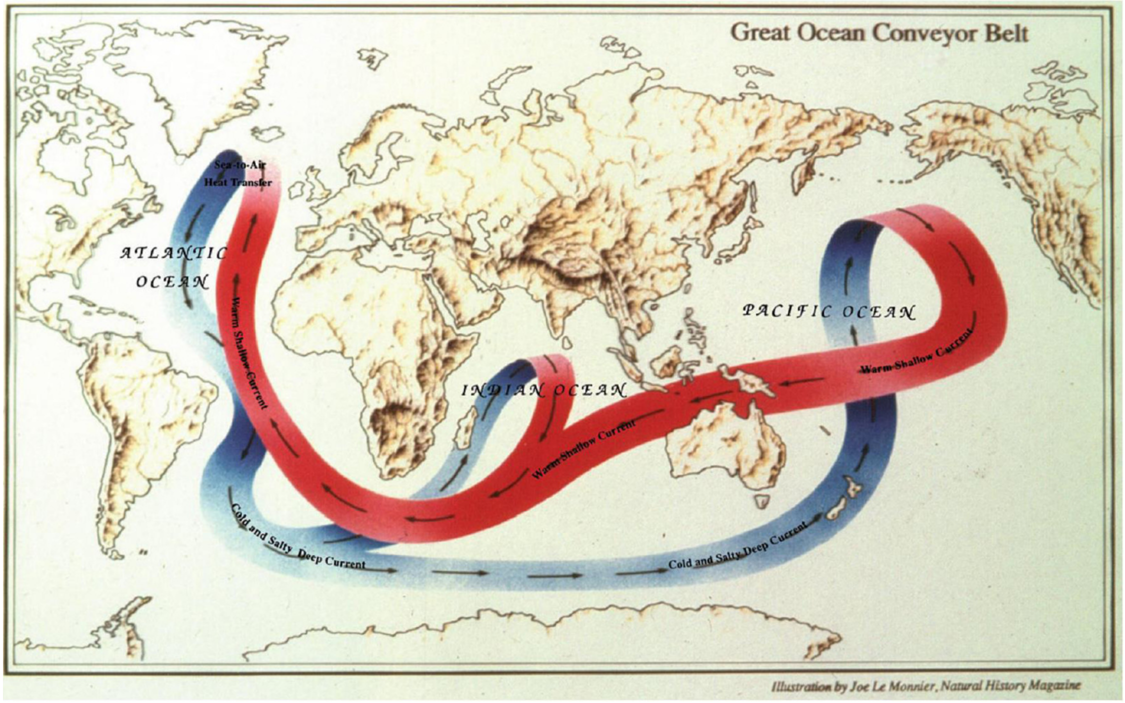

Fig. 5. The great ocean conveyor logo [156]. Illustration by Joe Le Monnier, Natural History Magazine. It is a simplified picture of the main ocean currents transporting heat around the globe.

4.2.4. Microdosing with ^{14}C for drug developments

After the pioneering experiment of Turteltaub et al. [151] demonstrating AMS measurements for low-level ^{14}C labeling of specific biomedically active compounds, the field really took off with the development of small AMS facilities as described in the accompanying article of Synal [34]. When these facilities became available, the pharma industry got interested to apply microdosing for drug developments [152,153]. The extreme sensitivity of AMS allowed one to study the metabolism of new drugs in vivo in humans, considerably shortening the time to develop a new drug and leading to large savings. There remains, though, the question to what extend microdosing can test a new drug for therapeutic use, when much higher doses of a new drug have to be administered.

4.3. Hydrosphere

It is well known that our Earth is the only planet in the solar systems which harbors liquid water through most of its 4.5-billion year history. At the present time – and probably throughout the Holocene (the last 10,000 years) – the distribution of water on Earth is estimated to be: ocean 97.3%, ice sheets 2.1%, groundwater 0.6% [126]. More than two thirds of the surface of the Earth is covered by the oceans, and the transport of heat around the globe by the oceans is roughly of the same magnitude as the one transported by the atmosphere. This clearly has a strong impact on the climate. Another area of great interest in hydrology is the freshwater sources on Earth. Here groundwater investigations play a particularly important role. In the following, a few examples of these two areas will be given.

4.3.1. ^{14}C and other radionuclides in the ocean

Radionuclides, and particularly ^{14}C, are “Tracers in the Sea” [154], allowing a multitude of investigations to study the oceans [155]. One of the most attractive features which came out of these studies, when large water samples (~250 L) still had to be used for ^{14}C decay counting, is the great ocean conveyor depicted in Fig. 5 [156,157].

This idealized picture was later refined [158], but we are still far away from getting a comprehensive picture of the dynamics of the oceans. A big step forward was AMS, where measurements of ^{14}C in ocean water allowed one to reduce the sample size from 250 to 0.5 L, and well over 13,000 water samples were measured within the World Ocean Circulation experiment (WOCE) project in the 1990s at the National Ocean Science AMS facility (NOSAMS) in Woods Hole [159]. By now the number of ^{14}C measurements in ocean water samples has surely surpassed 20,000. The analysis of this enormous bulk of data is being undertaken by dedicated oceanographers leading to a better understanding of ocean currents in three dimensions [160].

A radionuclide of great interest for oceanography is ^{39}Ar, which was measured by low level counting as long as large ocean water samples were taken [161]. The half-life of ^{39}Ar (269 year) is well matched to global water movements around the globe (500–2000 year), but low level counting ceased with the small sample taking triggered by AMS. Successful AMS measurements at the ATLAS linac at Argonne National Lab have been undertaken to measure the very low isotope ratios of ^{39}Ar/^{40}Ar ($<8 \times 10^{-16}$) in argon extracted from ocean water samples [162]. But eventually it turned out that these measurements are too sensitive to the ^{39}K isobar interference which cannot be consistently controlled to the level required for these ultra-low isotope ratio measurements, despite big efforts [163].

Releases from nuclear reprocessing provide radionuclides suited for studying ocean circulation. This includes ^{129}I studied in the Norwegian Sea [164], ^{99}Tc [165], and ^{237}Np [166]. Recently, Fallout of ^{236}U from the nuclear weapons testing period is also showing promise to be used as an oceanic tracer [167].

4.3.2. Groundwater dating

Groundwater is a natural resource of great importance for providing freshwater to many places on Earth. Similar to oil, fossil groundwater is a limited resource, and age determinations allow one to gain information on recharging times. An example for identifying short recharge times is to measure the ^{14}C bomb peak in young stalagmites growing in areas of freshwater supply [168]. In the case of the Wombeyan cave near Sydney, the time shift of the ^{14}C bomb peak indicates a recharging time of only six years for this important freshwater source. If one employs natural ^{14}C and ^{36}Cl to ground water dating, more complex hydrologies can be deciphered such as the one in the Palm Valley of central Australia [169].

Of particular interest to hydrology are large aquifers in the world with very old groundwater. An example is the Great Artisean Basin (GAB) in Australia, which has been first investigated with ^{129}I [170] and ^{36}Cl [171], indicating groundwater ages of more than 100,000 years. Since dating with both radionuclides is problematic because of unknown underground contributions, groundwater dating in the GAB was performed with ^{81}Kr, an almost ideal tracer for this purpose. AMS measurements were performed at the National Superconducting Cyclotron Laboratory at Michigan State University, and groundwater ages in the range from 200,000 to 400,000 were established [118]. It is interesting to note, that ^{81}Kr dating of old groundwater in the range from 0.5 to 1 million year has also been performed with the laser-based ATTA technique (Atom Trap Trace Analysis) in the Nubian aquifer of the Western Egypt Desert [172]. One also hopes to develop ATTA for ^{39}Ar [173,174], which would be particularly important for dating younger ground waters. Since both noble gas radionuclides are extremely difficult to measure with AMS, ATTA is likely to develop into the method of choice [175].

4.4. *Cryosphere*

After a prolonged ice-free period on Earth during the Mesozoic (225–65 million years ago), first ice may have started to form in Antarctica some 30 million years ago [176]. During the Pleistocene (2.5–0.01 million years ago), the ice sheets as we know them today dominated the polar regions of Greenland and Antarctica. However, this period is characterized by a sequence of colder (glacial) and warmer (interglacial) periods driven largely by the variation of three orbital Earth parameters (excentricity, obliquity, precision), which in turn determine the strength of the solar insulation [177–179]. During glacial times the land-locked ice mass increased roughly by a factor of two [126], lowering the sea level worldwide by about 100 m. Polar ice sheets are a rich archive of climatic conditions on Earth, with ^{18}O/^{16}O and D/H isotope ratios providing a useful proxy for past temperatures [180,181].

The longest cores from Antarctica reach back about 800,000 years (Fig. 6, see also Section 4.4.2). This figure from the EPICA collaboration [182] reveals interesting information about climatic conditions on the Earth during this time period. One of the striking features is the change of a ~40,000-year periodicity of warm periods (interglacials) before 500,000 years ago to about 100,000 years thereafter. Even though the variation of the solar insulation [179] shown in the top panel of Fig. 6 must have some influence on the climate, the observed periodicity is probably influenced by additional factors not yet well understood.

4.4.1. *^{10}Be record in Greenland ice cores*

Although a number of cosmogenic radionuclides (^{10}Be, ^{14}C, ^{26}Al, ^{36}Cl, ^{41}Ca, ^{129}I) have been measured in ice cores of Greenland, ^{10}Be provides the most useful proxy of paleoclimatic studies [185]. The residence time of ^{10}Be in the troposphere is short (a few weeks), and the relatively high production rate (cf. Fig. 3) result in concentrations in the range of 10^7 ^{10}Be atoms per kg ice. Since little ^{9}Be is present in ice cores, a known amount of ^{9}Be carrier can be added for AMS measurements to determine accurate ^{10}Be/^{9}Be ratios, and thus the ^{10}Be concentration in ice. The ^{10}Be record in ice has also been used to reconstruct solar modulation throughout the Holocene [186].

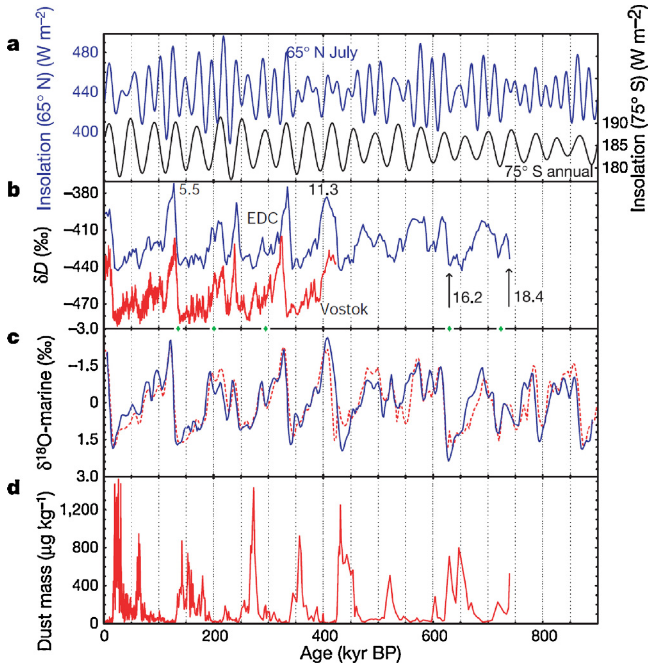

Fig. 6. Comparison of EPICA Dome C data with other paleoclimatic records. The figure is reproduced from Ref. [182], and a more detailed description can be found there. The upper panel (a) shows the record of the insolation at high northern and southern latitude [179]. The second panel (b) gives the temperature record as measured with the δD signal in the EPICA Dome C and the Vostok ice cores (red curve), respectively. The numbers refer to Marine Isotope Stages, where odd numbers are assigned to warm periods and even ones to cold periods [183]. The third panel (c) gives two marine δ^{18}O signals from deep sea sediment cores, which reflect both temperature and ice mass changes [184]. The lowest panel (d) shows the dust signal, which is particularly large during cold periods. (For interpretation of the references to colour in this figure legend, the reader is referred to the web version of this article.)

4.4.2. *Antarctica*

While the Greenland ice core record reaches back at most 200,000 years, the deepest ice cores in Antarctica approach 800,000 years [182]. We do, in fact, not know what the oldest ice on Earth is, because so far only indirect methods were used to determine some supposedly very old ice in the Dry Valleys of Antarctica. Sugden et al. [187] inferred an age of 8.1 million years from ^{40}Ar/^{39}Ar dating of a thin ash layer on top of till-covered ancient ice. Schaefer et al. [188] found a minimum age of 2.3 million years from cosmogenic helium and neon measured in rock surfaces of eratics on the till. A few attempts to develop long-lived radionuclides as direct chronometers to date old ice have been reported. AMS measurements of the ^{26}Al/^{10}Be atom ratio in ice is a promising possibility [133], although the low production rate of ^{26}Al in the atmosphere (Fig. 3) combined with a low yield of negative Al ions requires relatively large ice volumes (~20 kg) to obtain statistically significant results. ^{81}Kr would be another useful radionuclide to date old ice, however the concentration is exceedingly low (~1000 atoms per kg ice), and only one measurement with laser resonance ionization mass spectrometry was once performed on 224 kg of blue ice from the Antarctic mountains [189]. There is some promise of recent developments of ATTA to reduce the amount of ice required for a ^{81}Kr measurements considerably [175].

4.4.3. *Glacial changes*

Although the Holocene is considered to be an interglacial with relatively stable temperatures, glaciers covering high-altitude mountains are sensitive to small climate changes. The waxing and waning of glaciers leaves datable moraines behind which can be used as indicators for these movements. An example is given for a glacier near Mount Cook in New Zealand [190], where exposure dating of moraines with ^{10}Be (see Section 4.5) indicates considerable fluctuation throughout the Holocene. These fluctuations seem not to be synchronous with fluctuations of glaciers in the northern hemisphere [190], indicating that regional effects may influence those smaller climate changes.

Glacial fluctuations in the Latest Pleistocene and Holocene in Europe are discussed in a review article of Ivy-Ochs et al. [191]. A reduced length of the Rhone glacier through most of the Holocene was found with a new ^{14}C/^{10}Be exposure dating method [192]. Similar results had been reported from the Pasterze Glacier in the Austrian Alps [193]. Since Alpine glaciers usually move fast, it is difficult to find old ice. However, a study of ^{14}C in the organic fraction of small carbonaceous aerosols in a high-altitude glacier of the Monta Rosa mountains in Switzerland revealed a late Pleistocene age of the oldest ice near the bedrock [194].

A unique effort to develop AMS measurements of the relatively short-lived radionuclide ^{32}Si ($t_{1/2} = 144$ year) for ice dating in the range of 1000 years is being pursued by Morgenstern et al. [195]. Here the technical challenge is the separation of the overwhelming isobaric background of stable ^{32}S, which is accomplished by the gas-filled magnetic spectrograph technique [39] at a large tandem accelerator [195]. Other potential applications of ^{32}Si are discussed elsewhere [47].

4.5. Lithosphere

Solid surfaces on Earth (e.g. rocks) are exposed to secondary cosmic radiation comprising a nucleonic and muonic component, which induce nuclear reactions. The resulting build-up of radionuclides such as ^{10}Be, ^{14}C, ^{26}Al, ^{36}Cl can be used for surface exposure dating of fresh rock surfaces [196], and erosion studies as well [197]. A comprehensive review of the field can be found in Gosse and Phillips [198].

4.5.1. Surface exposure dating and geomorphological studies

Dating of moraines and rock surfaces exposed after the retreat of glaciers are examples mentioned in Section 4.4.3. Exposure dating with ^{10}Be and ^{26}Al produced in quartz has been applied in a detailed geomorphological study in the northwestern Himalayas [199]. In this study the incision rate of the Indus river could be obtained by combining the exposure time of abandoned river terraces with the height of these terraces above the current river surface. In order to obtain accurate exposure times the production rates of particular radionuclides have to be known. Since these depend on latitude and altitude, there is an ongoing debate about the correct values for the production rates. Recent ^{10}Be measurements to study denudation rates in the Himalayas [200] list many relevant references for this debate.

A fairly recent addition to surface studies is ^{53}Mn, which is mainly produced from the Fe content in rocks. The AMS measurements requires large tandem accelerators to separate the isobaric interference of ^{53}Cr. Due to the fairly long half-life of 3.7 million years, it allows surface dating of up to about10 million years [201,202].

4.5.2. Paleoclimatic studies in loess

Loess is a rather common sedimentary deposit of aeolian origin, with particularly large and ancient deposits in China (~0.5 million km^2, up to 400 m thick). The study of loess–paleosol sequences with ^{10}Be and geomagnetic methods allows one to draw conclusions about the paleoclimate. A 130,000-year record of two loess profiles (12 and 15 m length, respectively) from China has been analyzed in this way [203]. Since much thicker loess deposits exist in China, this opens the possibility to extend the method much further back in time (~2.5 million years). This would allow one to obtain information on the paleoclimate in this part of the world during the entire Pleistocene.

4.5.3. Burial dating

With the appropriate geological setting, buried sediments can be dated up to 5 million years through the decrease of the ^{26}Al/^{10}Be ratio originally produced when a quartz-containing sediment was exposed to cosmic secondary radiation on the surface [204]. The initial ^{26}Al/^{10}Be ratio is about 6, and first attempts at burial dating measurements in sediments and flints from the Tabun cave of Israel indicated the basic usefulness of the methods provided the proper material can be retrieved from an archeologically interesting context [205]. This method has now been successfully applied to date sediments around an early hominid, the famous Peking man, to an age of 0.77 ± 0.08 million years, appreciably older than previously known [206].

4.6. Cosmosphere

This domain includes extraterrestrial material, which somehow reaches the Earth by natural processes (e.g. meteorites, cosmic radiation) or through artificial means (lunar material). Meteorites typically spend millions of years in space outside the influence of terrestrial and solar magnetic fields. They are therefore continuously exposed to the full intensity and energies of primary cosmic rays, leading to secular equilibrium of a variety of radionuclides. The production of radionuclides in meteorites has been investigated both theoretically [207] and experimentally [208]. The surface of the moon, which lacks an atmosphere and a magnetic field is a perfect target for solar cosmic rays, including also the low-energy end of the cosmic ray spectrum.

4.6.1. Terrestrial ages of meteorites

Since the equilibrium concentration of a particular radionuclide can be measured in recent falls, terrestrial ages can be determined from the decrease of the concentration of a radionuclide whose half-life is known. In this way terrestrial ages for Antarctic meteorites were determined from AMS measurements of ^{36}Cl [209]. An interesting application of these meteorites was the determination of the half-life of ^{41}Ca by measuring both ^{41}Ca and ^{36}Cl concentrations for meteorites of different terrestrial age. With the known half-life of ^{36}Cl $(3.01 \pm 0.02) \times 10^5$ year, a half-life of $(1.03 \pm 0.07) \times 10^5$ year could be inferred from these measurements for ^{41}Ca [210]. This half-life is consistent with the recent high-precision measurement given in Table 1.

4.6.2. Measurements of ^{59}Ni on the moon

Soft components of cosmic rays can only produce reaction products at the very surface of meteorites. Since the outer layers of a meteorite are ablated by their fiery entry into the Earth's atmosphere, the information gets lost. This is different for lunar surface rocks, which have therefore been studied to obtain this special information of cosmic rays. In particular, the flux of low-energy solar alpha particles has been studied by measuring a near-surface profile of ^{59}Ni in lunar rocks produced via the reaction ^{56}Fe(α,n)^{59}Ni [211,212]. Since the exposure age of the lunar rocks determined from Kr isotope measurements turned out to be ~2 million years, ^{59}Ni with a half-life of 76,000 years (Table 1) can be assumed to be in secular equilibrium with its production rate (cf. Eq. (1) in Section 4.1).

4.6.3. Live supernova remnants on earth?

AMS allows one to search for extremely low abundances of particular nuclides, which may exist in terrestrial materials only due to the input of very rare events such as a "near-by" supernova explosion. Here, it is important that other production mechanisms (cosmic rays, spontaneous and induced fission, anthropogenic sources) can be excluded. So far, evidence for such a supernova explosion some 3 million years ago was found only for one radionuclide, ^{60}Fe, in a deep sea ferromanganese crust from the South Pacific [213–215]. Efforts to confirm this signal in other materials [216], and to look for ^{244}Pu as well, are under way.

4.6.4. Presolar grains

Primitive meteorites contain small grains with isotopic compositions which deviate substantially from the average solar system isotopic composition of the elements [217]. It is thus assumed that these represent materials which were not subject to the averaging procedure of the early solar nebula. Since the particular isotopic signatures of these grains are fingerprints of the stellar processes they originate from, it is of particular interest to obtain isotopic compositions of heavy elements. Since heavy elements exist only in trace amounts in these grains, an AMS study was performed at VERA to measure stable platinum isotopes in presolar nanodiamonds [218]. Although an enhancement of the ^{198}Pt/^{195}Pt isotope ratio as compared to the solar system abundance was observed for the first time, the result was somewhat marginal and clearly needs confirmation through more systematic studies.

4.6.5. Geochemical solar neutrino detection

The mystery of the reduced flux of solar neutrinos observed in the ^{37}Cl experiment [3] has been solved by the discovery of neutrino oscillations [219]. However, this and other experiments can only measure the present-day solar neutrino flux from the sun. To integrate over a longer period, the production of a long-lived radionuclide by solar neutrinos would be useful [220]. A case of considerable interest is ^{205}Pb with a half-life of 17 million years (Table 1), which can be produced by the inverse beta decay of $^{205}\mathrm{Tl}(\nu,\mathrm{e}^-)^{205}\mathrm{Pb}$ [221]. Great strides to develop an AMS method for ^{205}Pb and to find the appropriate thalium mineral have been made [222–224] but so far no definite project evolved. Other radionuclides such as ^{97}Tc and ^{98}Tc have also been proposed [225], and preliminary attempts to isolate these radionuclides from a molybdenum ore have been reported [226]. Similar to the detection of radionuclides from supernova remnants described in the previous section, also in this case one must be sure that any production process other than the one induced by solar neutrinos can be excluded.

4.6.6. Search for superheavy elements in nature

Ever since the intriguing prediction that an 'island of stability' may exist around $A \sim 300$ beyond the heaviest known nuclides, the search to find superheavy elements (SHE) in nature was pursued on various avenues [227,228] (see also a reminiscent article by Armbruster and Münzenberg [229]). An early AMS search in a Pt placer nugget [230] set limits of 10^{-11} for a SHE nuclide, ^{294}110, provided that the half-life was about 100 million years and its stellar abundance relative to platinum was 0.03 when the solar system formed [231]. Until today no confirmed evidence for SHEs in nature was found. However, the group of A. Marinov et al. recently reported positive evidence from high-resolution inductively coupled sector field mass spectrometry (ICP-SF-MS) for neutron deficient Th isotopes [232], neutron deficient Rg isotopes in gold [233], and a SHE nuclide with $A = 292$ and $Z \sim 122$ in thorium [234]. This triggered extensive AMS experiments at the 14-MV tandem accelerator in Munich [235,236], and at the 3-MV VERA facility in Vienna [237–239]. None of the Marinov results were confirmed with AMS, with abundance limits several orders of magnitude below the one of the ICP-SF-MS experiments. The results are summarized in Fig. 7.

4.7. Technosphere

Man-made radionuclides came into use with the advent of accelerators in the 1930s, and nuclear reactors and nuclear weapons in the 1940s. They play a particularly important role in nuclear medicine (e.g. ^{11}C, ^{18}F, ^{60}Co, ^{81}Kr, $^{99\mathrm{m}}$Tc, ^{123}I, ^{202}Tl), but also in a variety of technological applications. Sometimes releases of radionuclides happened, which modified significantly their respective natural budget. The most obvious event was the above-ground nuclear weapons testing period (1950–1963), which increased ^{14}C in the atmosphere by a factor of two (see Section 4.2.2). Releases from nuclear fuel reprocessing plants (^{99}Tc, ^{129}I), and fallout from the weapons tests (^{236}U) are being used as oceanographic tracers (see Section 4.3.1). In the following, we want to discuss a few laboratory applications, where AMS measurements of artificially produced radionuclides are being used.

4.7.1. Half-life measurements

Long half-lives are notoriously difficult to measure, which is reflected by the considerable uncertainty of this basic property for some of the radionuclides listed in Table 1. AMS measurements have contributed to half-life measurements, albeit with relatively large uncertainties because absolute isotope ratio measurements are required. Examples are ^{32}Si [241,242], ^{44}Ti [243], ^{60}Fe [56,244], ^{126}Sn [96,97], ^{146}Sm [38]. In all cases, the stable isobar separation was the crucial contribution of the AMS measurements.

4.7.2. Studies related to nuclear fusion

Great strides are being made to develop nuclear fusion for energy generation, but the realization of a nuclear fusion power plant for electricity generation still lies decades away as indicated in the recent Roadmap to Fusion Energy by the European Fusion Development Agreement [245].

A few studies related to fusion have been performed with AMS. Tritium depth profiling in carbon tiles from a fusion experiment were performed with a small AMS facility at Rossendorf [246]. The cross section of the $^{27}\mathrm{Al}(\mathrm{n},2\mathrm{n})^{26}\mathrm{Al}$ reaction near threshold is sensitive to the thermal distribution of neutrons from the $^{3}\mathrm{H}(^{2}\mathrm{H},\mathrm{n})^{4}\mathrm{He}$ reaction and could thus be used to determine the temperature of the fusion plasma. To this end ^{26}Al was measured with AMS in Al foils irradiated with 14-MeV neutrons around the reaction threshold [247].

4.7.3. Reaction studies for nuclear astrophysics

The description of the synthesis of elements in stars require cross sections for a multitude of nuclear reactions under different stellar conditions [248]. A number of these reactions have been studied in the laboratory, and if long-lived radionuclides are produced, they can be measured with AMS [249,250]: $^{9}\mathrm{Be}(\mathrm{n},\gamma)^{10}\mathrm{Be}$, $^{13}\mathrm{C}(\mathrm{n},\gamma)^{14}\mathrm{C}$, $^{14}\mathrm{N}(\mathrm{n},\mathrm{p})^{14}\mathrm{C}$, $^{25}\mathrm{Mg}(\mathrm{p},\gamma)^{26}\mathrm{Al}$, $^{26}\mathrm{Mg}(\mathrm{p},\mathrm{n})^{26}\mathrm{Al}$, $^{33}\mathrm{S}(\alpha,\mathrm{p})^{36}\mathrm{Cl}$, $^{36}\mathrm{S}(\mathrm{p},\mathrm{n})^{36}\mathrm{Cl}$, $^{40}\mathrm{Ca}(\mathrm{n},\gamma)^{41}\mathrm{Ca}$, $^{40}\mathrm{Ca}(\alpha,\gamma)^{44}\mathrm{Ti}$, $^{54}\mathrm{Fe}(\mathrm{n},\gamma)^{55}\mathrm{Fe}$, $^{58}\mathrm{Ni}(\mathrm{n},\gamma)^{59}\mathrm{Ni}$, $^{62}\mathrm{Ni}(\mathrm{n},\gamma)^{63}\mathrm{Ni}$, $^{70}\mathrm{Ge}(\mathrm{n},3\mathrm{n})^{68}\mathrm{Ge}$, $^{147}\mathrm{Sm}(\mathrm{n},2\mathrm{n})^{146}\mathrm{Sm}$, $^{204}\mathrm{Pb}(\mathrm{n},3\mathrm{n})^{202}\mathrm{Pb}$, $^{209}\mathrm{Bi}(\mathrm{n},\gamma)^{210\mathrm{m}}\mathrm{Bi}$, $^{232}\mathrm{Th}(\mathrm{n},2\mathrm{n})^{231}\mathrm{Th}\ (\beta^-)\ ^{231}\mathrm{Pa}$, $^{232}\mathrm{Th}(\mathrm{n},3\mathrm{n})^{230}\mathrm{Th}$.

Under explosive nuclear conditions (e.g. supernovae), high neutron fluxes at high temperatures occur, and several of the neutron-induced reactions above have been studied by irradiating appropriate targets with a Maxwellian thermal neutron distribution corresponding to the temperature of interest [251]. AMS studies for nuclear astrophysics is an evolving field, with many more reactions to be studied when the new generation of neutron generators such as FRANZ in Frankfurt come online [252], promising a hundredfold increase in neutron flux as compared to previously available neutron sources.

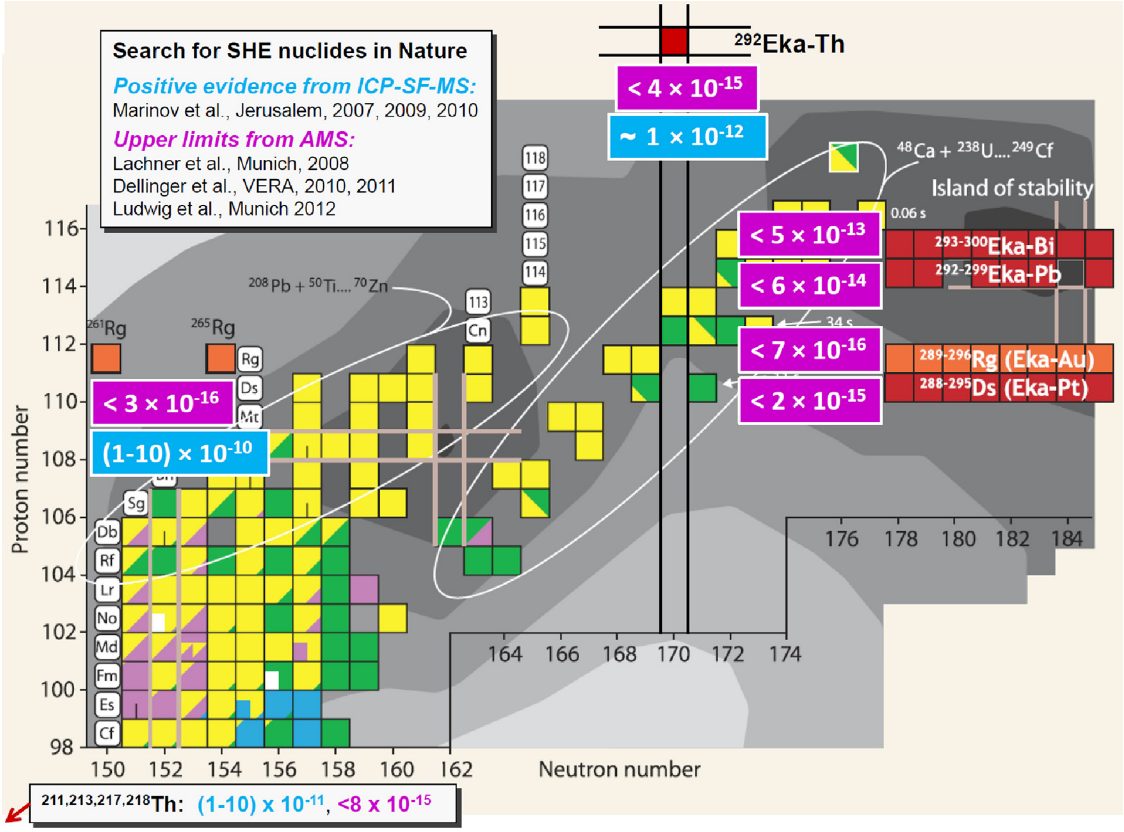

Fig. 7. Summary of the results for searches of superheavy elements in nature. The basic layout of the figure is from Stoyer [240], depicting the upper end of the chart of nuclides. The shades of gray in the background indicate the relative stability of nuclides due to shell model corrections (darker means more stable). Nuclides marked in orange and red have been measured with AMS. Abundance limits are indicated in the violet boxes. The positive evidence of Marinov et al. are marked in blue boxes. (For interpretation of the references to colour in this figure legend, the reader is referred to the web version of this article.)

4.7.4. *Neutron dosimetry of the Hiroshima bomb*

Survivors of the Hiroshima and Nagasaki bomb explosion constitute the only group of people to study long-time health effects of the exposure to neutron radiation [253]. In order to improve the information about the radiation fields, long-lived radioisotopes have been measured with AMS in suitable materials. For the thermal neutron dose in Hiroshima, the first ^{36}Cl and ^{41}Ca concentrations were measured in granite stones [254]. Later more extensive studies of ^{36}Cl were performed in granite [255,256], and of ^{41}Ca in tooth enamel of atom bomb survivors [257,258]. The fast neutron flux was measured with ^{63}Ni in copper samples [259]. These measurements are part of an effort to establish the correct neutron dose produced by the atom bomb explosions.

4.7.5. *Nuclear safeguards*

Nuclear safeguards need a variety of measuring technique to comprehensively cover the field, and AMS can make significant contributions. A good example is the determination of the ^{240}Pu/^{239}Pu atom ratio, which is a fingerprint for the origin of the plutonium. Low ratios (~0.1) indicate weapons plutonium, and higher ratios (~0.4) reactor plutonium [260]. As the alpha-decay energies of these two isotopes are very similar, it is not possible to determine this ratio from alpha spectroscopy [261]. Another sensitive indicator is the ^{236}U/^{238}U ratio, which is orders of magnitude higher for uranium from nuclear reactors as compared to weapons fallout [262]. Since there are no stable atomic isobars interfering with actinides, AMS measurements can also be performed with the new generation of small AMS facilities [34].

An interesting new idea about fingerprinting nuclear fuel with AMS measurements of samarium isotopes is discussed by the group from Livermore [263]. The isotopic abundances of ^{146}Sm, ^{149}Sm, and ^{151}Sm allow one to determine the operating conditions under which a nuclear reactor was running. It is argued that AMS should be capable to perform measurements at samarium isotope concentrations too low to be measured with ICP-MS.

5. Future developments

Three technical developments will further advance applications of AMS:

1. New methods of selective isobar suppression of negative ions at the injection side of AMS facilities are being developed. Laser interaction with negative ion beams at very low energy allows one to detach electrons selectively from unwanted negative ions [40,264]. An alternative method to remove unwanted negative ion species is selective chemistry in reaction cells [42,43,265]. It is thus likely that essentially all long-lived radionuclides which form negative atomic or molecular ions will eventually become available for AMS measurements.
2. The development of ever smaller AMS facilities for radiocarbon dating [34], will possibly make those facilities also attractive for other radionuclides when combined with the novel methods for low-energy isobar suppression mentioned above.
3. For radiocarbon measurements, the reduction of sample sizes from milligram to microgram has been achieved at several laboratories, e.g. [146,192,266]. In addition, direct use of CO_2 in a gas ion source avoids the graphitization step in radiocarbon sample preparation [267], and also allows for compound specific radiocarbon analysis [268].

6. Conclusion

The multitude of applications touched upon in this review demonstrate the versatility of AMS, which allows one to enter any field where the ultra-sensitive analysis of long-lived radionuclides is of interest. The future developments mentioned above will undoubtedly expand the range of applications further by making more radionuclides available for AMS. In addition, the truly interdisciplinary – and often cross-disciplinary – character of AMS applications suggests that all embracing studies of natural sciences including sometimes the humanities are possible.

Acknowledgements

The author benefitted from countless discussions with colleagues from AMS and other fields to comprehend the full range of AMS applications. Discussions on the manuscript with Robin Golser are gratefully acknowledged.

References

[1] G.J. Wasserburg, M. Busso, R. Gallino, K.M. Nollett, Short-lived nuclei in the early solar system: possible AGB sources, Nuclear Physics A 777 (2006) 5–69.
[2] H. Hintenberger, High-sensitivity mass spectroscopy in nuclear studies, Annual Review of Nuclear Science 12 (1962) 435–506.
[3] B.T. Cleveland, T. Daily, R. Davis Jr., J.R. Distel, K. Lande, C.K. Lee, P.S. Wildenhain, J. Ullmann, Measurement of the solar electron neutrino flux with the Homestake chlorine detector, The Astrophysical Journal 496 (1998) 505–510.
[4] H. Oeschger, J. Houtermans, H. Loosli, M. Wahlen, The constancy of cosmic radiation from isotope studies in meteorites and on Earth, in: I.U. Olsen (Ed.), 12th Nobel Symposium on Radiocarbon variation and Absolute Chronology, John Wiley & Sons, New York, 1970, pp. 471–498.
[5] M. Anbar, The limitation of mass spectrometric radiocarbon dating using CN^- ions, in: H.E Gove (Ed.), Edating with Accelerators, University of Rochester, Rochester, 1978, pp. 152–156.
[6] R.A. Muller, Radioisotope dating with a cyclotron, Science 196 (1977) 489–494.
[7] K.H. Purser, R.B. Liebert, A.E. Litherland, R.P. Beukens, H.E. Gove, C.L. Bennet, H.R. Clover, W.E. Sondheim, An attempt to detect stable N^- ions from a sputter ion source and some implications of the results on the design of tandems for ultrasensitive carbon analysis, Revue de Physique Appliquée 12 (1977) 1487–1492.
[8] D.E. Nelson, R.G. Korteling, W.R. Stott, Carbon-14: direct detection at natural concentrations, Science 198 (1977) 507–508.
[9] C.L. Bennet, R.P. Beukens, M.R. Clover, H.E. Gove, R.B. Liebert, A.E. Litherland, K.H. Purser, W.E. Sondheim, Radiocarbon dating using electrostatic accelerators: negative ions provide the key, Science 198 (1977) 508–510.
[10] L.W. Alvarez, He^3 in helium, Physical Review 56 (1939) 379.
[11] L.W. Alvarez, R. Cornog, Helium and hydrogen of mass 3, Physical Review 56 (1939) 613.
[12] H.A. Bethe, R.F. Bacher, Nuclear physics A. Stationary states of nuclei, Reviews of Modern Physics 8 (1936) 82–229.
[13] L.W. Alvarez, The early days of accelerator mass spectrometry, Physics Today 35 (1) (1982) 25–32.
[14] Y. Yamaguchi, Possible use of ^{41}Ca in nuclear dating, Progress in Theoretical Physics (Japan) 30 (1963) 567.
[15] G.M. Raisbeck, F. Yiou, Possible use of ^{41}Ca for radioactive dating, Nature 277 (1979) 42–44.
[16] W. Henning, W.A. Bell, P.J. Billquist, B.G. Glagola, W. Kutschera, Z. Liu, H.F. Lucas, M. Paul, K.E. Rehm, J.L. Yntema, Calcium-41 concentration in terrestrial materials: prospects for dating of Pleistocene samples, Science 236 (1987) 725–727.
[17] D. Fink, ^{41}Ca: past, present and future, Nuclear Instruments and Methods in Physics Research B 52 (1990) 572–582.
[18] R.A. Muller, Radioisotope dating with accelerators, Physics Today (1979) 23–30, February.
[19] A.E. Litherland, Ultrasensitive mass spectrometry with accelerators, Annual Review of Nuclear and Particle Science 30 (1980) 437–473.
[20] D. Elmore, F.M. Phillips, Accelerator mass spectrometry for measurement of long-lived radioisotopes, Science 236 (1987) 543–550.
[21] W. Kutschera, Accelerator mass spectrometry: a versatile tool for research, Nuclear Instruments and Methods in Physics Research B 50 (1990) 252–261.
[22] W. Kutschera, M. Paul, Accelerator mass spectrometry in nuclear physics and astrophysics, Annual Review of Nuclear and Particle Science 40 (1990) 411–438.
[23] R.C. Finkel, M. Suter, AMS in the earth sciences, Advances in Analytical Geochemistry 1 (1993) 1–114.
[24] L.K. Fifield, Accelerator mass spectrometry and its applications, Reports on Progress in Physics 62 (1999) 1223–1274.
[25] M. Suter, 25 years of AMS—a review of recent developments, Nuclear Instruments and Methods in Physics Research B 223–224 (2004) 139–148.
[26] P. Collon, W. Kutschera, Z.-T. Lu, Tracing noble gas radionuclides in the environment, Annual Review of Nuclear and Particle Science 54 (2004) 39–67.
[27] W. Kutschera, Progress in isotope analysis at ultra-trace level by AMS, International Journal of Mass Spectrometry 242 (2005) 145–160.
[28] A.J.T. Jull, G.S. Burr, Accelerator mass spectrometry: is the future bigger or smaller? Earth and Planetary Science Letters 243 (2006) 305–325.
[29] R. Hellborg, G. Skog, Accelerator mass spectrometry, Mass Spectrometry Reviews by Wiley Periodicals Inc. 27 (2008) 398–427.
[30] A.E. Litherland, X.-L. Zhao, W.E. Kieser, Mass spectrometry with accelerators, Mass Spectrometry Reviews by Wiley Periodicals, Inc. 30 (2010) 1037–1072.
[31] D. Fink, AMS-11 in Rome 2008: past achievements, current and future trends, Nuclear Instruments and Methods in Physics Research B 268 (2010) 1334–1342.
[32] C. Tuniz, J.R. Bird, D. Fink, G.F. Herzog, Accelerator Mass Spectrometry—Ultrasensitive Analysis for Global Science, CRC Press, Boca Raton, 1998, pp. 371.
[33] C. Zondervan, F. Prior, R. Bruhn, Sparks (Eds.), Proceedings of the twelfth international conference on accelerator mass spectrometry in Wellington (New Zealand), Nuclear Instruments and Methods in Physics Research B 294 (2013) 1–714.
[34] H.-A. Synal, Developments in Accelerator Mass Spectrometry, 2013, in this volume.
[35] R. Middleton, A review of ion sources for accelerator mass spectrometry, Nuclear Instruments and Methods B 5 (1984) 193–199.
[36] R. Middleton, A Negative-ion Cookbook, University of Pennsylvania, Philadelphia, 1989 (revised 1990) http://www.pelletron.com/cookbook.pdf
[37] W. Kutschera, M. Paul, I. Ahmad, T.A. Antaya, P.J. Billquist, B.G. Glagola, R. Harkewicz, M. Hellstrom, D.J. Morrissey, R.C. Pardo, K.E. Rehm, B.M. Sherrill, M. Steiner, Long-lived noble gas radionuclides, Nuclear Instruments and Methods in Physics Research B 92 (1994) 241–248.
[38] N. Kinoshita, M. Paul, Y. Kashiv, P. Collon, C.M. Deibel, B. DiGiovine, J.P. Greene, D.J. Henderson, C.L. Jiang, S.T. Marley, T. Nakanishi, R.C. Pardo, K.E. Rehm, D. Robertson, R. Scott, C. Schmitt, X.D. Tang, R. Vondrasek, A. Yokoyama, A shorter ^{146}Sm half-life measured and implications for ^{146}Sm–^{142}Nd chronology in the solar system, Science 335 (2012) 1614–1617.
[39] M. Paul, B.C. Glagola, W. Henning, J.G. Keller, W. Kutschera, Z. Liu, K.E. Rehm, B. Schneck, R. Siemssen, Heavy ion separation with a gas-filled magnetic spectrograph, Nuclear Instruments and Methods A277 (1989) 418–430.
[40] O. Forstner, P. Andersson, C. Diehl, R. Golser, D. Hanstorp, W. Kutschera, A. Lindahl, A. Priller, P. Steier, A. Wallner, Isobar suppression in AMS using laser photodetachment, Nuclear Instruments and Methods in Physics Research B 266 (2008) 4565–4568.
[41] M. Martschini, J. Rohlén, P. Andersson, R. Golser, D. Hanstorp, A.O. Lindahl, A. Priller, P. Steier, O. Forstner, Light induced suppression of sulfur in a cesium sputter ion source, International Journal of Mass Spectrometry 315 (2012) 55–59.
[42] J. Eliades, A.E. Litherland, W.E. Kieser, L. Cousins, S.J. Ye, X.-L. Zhao, Cl/S isobar separation using an on-line reaction cell for ^{36}Cl at low energy, Nuclear Instruments and Methods in Physics Research B 268 (2010) 839–842.
[43] J. Eliades, X.-L. Zhao, A.E. Litherland, W.E. Kieser, On-line ion chemistry for the AMS analysis of ^{90}Sr and ^{135,137}Cs, Nuclear Instruments and Methods in Physics Research B 294 (2013) 361–363.
[44] C. Vockenhuber, V. Alfimov, M. Christl, J. Lachner, T. Schulze-König, M. Suter, H.-A. Synal, The potential of He stripping in heavy ion AMS, Nuclear Instruments and Methods in Physics Research B 294 (2013) 382–386.
[45] L.L. Lucas, M.P. Unterweger, Comprehensive review and critical evaluation of the half-life of tritium, Journal of Research of the National Institute of Standards and Technology 105 (2000) 541–549.
[46] G. Korschinek, A. Bergmaier, T. Faestermann, U.C. Gerstmann, K. Knie, G. Rugel, A. Wallner, I. Dillmann, G. Dollinger, Ch. Lierse von Gostomski, K. Kossert, M. Maiti, M. Poutivtsev, A. Remmert, A new value for the half-life of ^{10}Be by heavy-ion elastic recoil detection and liquid scintillation counting, Nuclear Instruments and Methods in Physics Research B 268 (2010) 187–191.
[47] L.K. Fifield, U. Morgenstern, Silicon-32 as a tool for dating the recent past, Quaternary Geochronology 4 (2009) 400–405.
[48] N. Nica, J. Cameron, B. Singh, Nuclear data sheets for $A = 36$, Nuclear Data Sheets 113 (2012) 1–155.
[49] R.W. Stoenner, O.A. Schaeffer, S. Katcoff, Half-lives of Argon-37, Argon-39, and Argon-42, Science 148 (1965) 1325–1328.
[50] K. Kossert, E. Günther, LSC measurements of the half-life of ^{40}K, Applied Radiation and Isotopes 60 (2004) 459–464.
[51] G. Jörg, Y. Amelin, K. Kossert, Ch. Lierse v. Gostomski, Precise and direct determination of the half-life of ^{41}Ca, Geochimica et Cosmochimica Acta 88 (2012) 51–65.
[52] I. Ahmad, J.P. Greene, E.F. Moore, S. Ghelberg, A. Ofan, M. Paul, W. Kutschera, Improved measurement of the ^{44}Ti half-life from a 14-year long study, Physical Review C 74 (2006) 1–8, 065803.
[53] M. Honda, M. Imamura, Half-life of ^{53}Mn, Physical Review C 4 (1971) 1182–1188.
[54] H. Junde, Nuclear data sheets for $A = 55$, Nuclear Data Sheets 109 (2008) 787–942.
[55] K. Nishiizumi, R. Gensho, M. Honda, Half-life of ^{59}Ni, Radiochimica Acta 29 (1981) 113–116.

[56] G. Rugel, T. Faestermann, K. Knie, G. Korschinek, M. Poutivtsev, D. Schumann, N. Kivel, I. Günther-Leopold, R. Weinreich, M. Wohlmuther, New measurement of the ^{60}Fe half-life, Physical Review Letters 103 (2009) 1–4, 072502.

[57] I.L. Barnes, S.B. Garfinkel, W.B. Mann, Nickel-63: standardization, half-life and neutron-capture cross-section, The International Journal of Applied Radiation and Isotopes 22 (1971) 777–781.

[58] E.A. McCutchan, Nuclear data sheets for $A=68$, Nuclear Data Sheets 113 (2012) 1735–1870.

[59] P. Bienvenu, P. Cassette, G. Andreoletti, M.-M. Bé, J. Comte, M.-Ch. Lépy, A new determination of ^{79}Se half-life, Applied Radiation and Isotopes 65 (2007) 355–364.

[60] C.M. Baglin, Nuclear data sheets for $A=81$, Nuclear Data Sheets 109 (2008) 2257–2437.

[61] E. Browne, Nuclear data sheets for $A=90$, Nuclear Data Sheets 82 (1997) 379–546.

[62] C.M. Baglin, Nuclear data sheets for $A=93$, Nuclear Data Sheets 112 (2011) 1163–1389.

[63] E. Browne, J.K. Tuli, Nuclear data sheets for $A=99$, Nuclear Data Sheets 112 (2011) 275–446.

[64] Y. Tendow, Nuclear data sheets for $A=129$, Nuclear Data Sheets 77 (1996) 631–770.

[65] B. Singh, A.A. Rodionov, Y.L. Khazov, Nuclear data sheets for $A=135$, Nuclear Data Sheets 109 (2008) 517–698.

[66] E. Browne, J.K. Tuli, Nuclear data sheets for $A=137$, Nuclear Data Sheets 108 (2007) 2173–2318.

[67] B. Singh, Nuclear data sheets for $A=151$, Nuclear Data Sheets 110 (2009) 1–264.

[68] C. Vockenhuber, F. Oberli, M. Bichler, I. Ahmad, G. Quitté, M. Meier, A.N. Halliday, D.-C. Lee, W. Kutschera, P. Steier, R.J. Gehrke, R.G. Helmer, New half-life measurement of ^{182}Hf: Improved chronometer for the early solar system, Physical Review Letters 93 (2004) 1–4, 172501.

[69] S. Zhu, F.G. Kondev, Nuclear data sheets for $A=202$, Nuclear Data Sheets 109 (2008) 699–786.

[70] F.G. Kondev, Nuclear data sheets for $A=2005$, Nuclear Data Sheets 101 (2004) 521–662.

[71] E. Browne, Nuclear data sheets for $A=210$, Nuclear Data Sheets 99 (2003) 649–753.

[72] A. Artna-Cohen, Nuclear data sheets for $A=228$, Nuclear Data Sheets 80 (1997) 723.

[73] S.J. Goldstein, M.T. Murrell, R.W. Williams, Half-life of ^{229}Th, Physical Review C 40 (1989) 2793–2795.

[74] E. Browne, J.K. Tuli, Nuclear data sheets for $A=230$, Nuclear Data Sheets 113 (2012) 2113–2185.

[75] E. Browne, Nuclear data sheets for $A=215$, 219, 223, 227, 231, Nuclear Data Sheets 93 (2001) 763–1061.

[76] N.E. Holden, Total half-lives for selected nuclides, Pure and Applied Chemistry 62 (1990) (1990) 941–968.

[77] E. Browne, Nuclear data sheets for $A=232$, Nuclear Data Sheets 107 (2006) 2579–2648.

[78] B. Singh, J.K. Tuli, Nuclear data sheets for $A=233$, Nuclear Data Sheets 105 (2005) 109–222.

[79] N.E. Holden, Total and spontaneous fission half-lives for uranium, plutonium, americium and curium nuclides, Pure and Applied Chemistry 61 (1989) 1483–1504.

[80] I.M. Lowles, T.D. Mac Mahon, R.A.P. Wiltshire, D. Crossley, A.J. Fudge, The half-life of ^{237}Np, Nuclear Instruments and Methods in Physics Research 312 (1992) 339–345.

[81] F.E. Chukreev, V.E. Makarenko, M.J. Martin, Nuclear data sheets for $A=238$, Nuclear Data Sheets 97 (2002) 129–240.

[82] E. Browne, Nuclear data sheets for $A=239$, Nuclear Data Sheets 98 (2003) 665–800.

[83] B. Singh, E. Browne, Nuclear data sheets for $A=240$, Nuclear Data Sheets 109 (2008) 2439–2499.

[84] M.J. Martin, Nuclear data sheets for $A=241$, Nuclear Data Sheets 106 (2005) 89–158.

[85] Y.A. Akovali, Nuclear data sheets for $A=234$, Nuclear Data Sheets 103 (2004) 515–564.

[86] Y.A. Akovali, Nuclear data sheets for $A=250$, 254, 258, 262, 266, Nuclear Data Sheets 94 (2001) 131–225.

[87] H. Godwin, Half-life of radiocarbon, Nature 195 (1962) 984.

[88] D.E. Watt, D. Ramsden, H.W. Wilson, The half-life of carbon-14, International Journal of Applied Radiation and Isotopes 11 (1961) 68–74.

[89] I.U. Olsson, I. Karlén, A.H. Turnbull, N.J.D. Prosser, A determination of the half-life of C^{14} with a proportional counter, Arkiv för Fysik 22 (1962) 237–255.

[90] E.E. Hughes, W.B. Mann, The half-life of carbon-14: comments on the mass-spectrometric methods, International Journal of Applied Radiation and Isotopes 15 (1964) 97–100.

[91] F. Bella, M. Alessio, P. Fratelli, A determination of the half-life of ^{14}C, Il Nuovo Cimento 58B (1968) 232–246.

[92] Particle Data Group, R.M. Barnett, et al., Review of particle physics, Physical Review D 54 (1996) 1–720.

[93] E.A. Samworth, E.K. Warburton, G.A.P. Engelbertink, Beta decay of the ^{26}Al ground state, Physical Review C 5 (1972) 138–142.

[94] T.L. Norris, A.J. Gancarz, D.J. Rokop, K.W. Thomas, Half-life of ^{26}Al, Journal of Geophysical Research 88 (Suppl.) (1983) B331–B333.

[95] J.H. Thomas, R.T. Skelton, R.W. Kavanagh, Half-life of ^{26}Al, Physical Review C 30 (1984) 385–387.

[96] P. Haas, P. Gartenmann, R. Golser, W. Kutschera, M. Suter, H.-A. Synal, M.J.M. Wagner, E. Wild, G. Winkler, A new half-life measurement of the long-lived fission product ^{126}Sn, Nuclear Instruments and Methods in Physics Research B 114 (1996) 131–137.

[97] P. Haas, P. Gartenmann, R. Golser, W. Kutschera, M. Suter, H.-A. Synal, M.J.M. Wagner, E. Wild, G. Winkler, Erratum to: "A new half-life measurement of the long-lived fission product ^{126}Sn" [Nucl. Instr. Meth. B 114 (1996) 131–137], Nuclear Instruments and Methods in Physics Research B 117 (1996) 474.

[98] S. Zhang, J. Guo, A. Cui, D. Li, D. Liu, Measurement of the half-life of ^{126}Sn using a radiochemical method, Journal of Radioanalytical and Nuclear Chemistry 212 (1996) 93–99.

[99] F. Oberli, P. Gartenmann, M. Meier, W. Kutschera, M. Suter, G. Winkler, The half-life of ^{126}Sn refined by thermal ionization mass spectrometry measurements, International Journal of Mass Spectrometry 184 (1999) 145–152.

[100] S.A. Catlow, G.L. Troyer, D.R. Hansen, R.A. Jones, Half-life measurement of ^{126}Sn isolated from Hanford nuclear defense waste, Journal of Radioanalytical and Nuclear Chemistry 263 (2005) 599–603.

[101] P. Bienvenu, L. Ferreux, G. Andreoletti, N. Arnal, M.-C. Lépy, J. Comte1, M.-M. Bé, Determination of ^{126}Sn half-life from ICP-MS and gamma spectrometry measurements, Radiochimica Acta 97 (2009) 687–694.

[102] V.F. Hess, Über Beobachtungen der durchdringenden Strahlung bei sieben Freiballonfahrten, Physikalische Zeitschrift 13 (1912) 1084–1091.

[103] W.F. Libby, Atmospheric helium three and radiocarbon from cosmic radiation, Physical Review 69 (1946) 671–672.

[104] W. Kutschera, Radiocarbon dating coming of age, in: POS Proceedings of Science, 2012 http://pos.sissa.it/archive/conferences/160/003/Bormio2012_003.pdf

[105] P. Crutzen, My life with O_3, NO_x and other YZO_xs, in: B.G. Malmström (Ed.), Nobel Lectures in Chemistry 1991–1995, World Scientific Publishing Company, Singapore, 1997, pp. 189–242.

[106] E.C. Anderson, W.F. Libby, S. Weinhouse, A.F. Reid, A.D. Kirshenbaum, A.V. Grosse, Natural radiocarbon from cosmic radiation, Physical Review 72 (1947) 931–936.

[107] J. Arnold, W.F. Libby, Age determination by radiocarbon content: checks with samples of known age, Science 110 (1949) 678–680.

[108] W.F. Libby, Radiocarbon dating, in: Nobel Lectures in Chemistry 1942–1962, Elsevier Publishing Company, Amsterdam/London/New York, 1964, pp. 588–612.

[109] J. Masarik, J. Beer, An updated simulation of particle fluxes and cosmogenic nuclide production in the Earth's atmosphere, Journal of Geophysical Research: Atmospheres 114 (D11103) (2009) 1–9.

[110] J.A. Simpson, Neutrons produced in the atmosphere by the cosmic radiations, Physical Review 83 (1951) 1175–1188.

[111] W.-T. Chou, E.K. Warburton, B.A. Brown, Gamov–Teller beta-decay rates for $A<18$ nuclei, Physical Review C 47 (1993) 163–177.

[112] P.J. Reimer, M.G.L. Baillie, E. Bard, A. Bayliss, J.W. Beck, P.G. Blackwell, C. Bronk Ramsey, C.E. Buck, G.S. Burr, R.L. Edwards, M. Friedrich, P.M. Grootes, T.P. Guilderson, I. Hajdas, T.J. Heaton, A.G. Hogg, K.A. Hughen, K.F. Kaiser, B. Kromer, F.G. McCormac, S.W. Manning, R.W. Reimer, D.A. Richards, J.R. Southon, S. Talamo, C.S.M. Turney, J. van der Plicht, C.E. Weyhenmeyer, INTCAL09 and MARINE09 radiocarbon age calibration curves, 0–50,000 years cal BP, Radiocarbon 51 (4) (2009) 1111–1150.

[113] C. Bronk Ramsey, R.A. Staff, C.L. Bryant, F. Brock, H. Kitagawa, J. van der Plicht, G. Schlolaut, M.H. Marshall, A. Brauer, H.F. Lamb, R.L. Payne, P.E. Tarasov, T. Haraguchi, K. Gotanda, H. Yonenobu, Y. Yokoyama, R. Tada, T. Nakagawa, A complete terrestrial radiocarbon record for 11.2 to 52.8 kyr B.P, Science 338 (2012) 370–374.

[114] M. Stuiver, H.A. Polach, Discussion reporting of ^{14}C data, Radiocarbon 19 (3) (1977) 355–363.

[115] W. Kutschera, Conference summary: trends in AMS, Nuclear Instruments and Methods in Physics Research B 123 (1997) 594–598.

[116] D. Lal, B. Peters, Cosmic ray produced radioactivity on the Earth, in: K. Sitte (Ed.), Handbuch der Physik, vol. 46 (2), 1967, pp. 551–612.

[117] H.H. Loosli, A dating method with ^{39}Ar, Earth and Planetary Science Letters 63 (1983) 51–62.

[118] P. Collon, W. Kutschera, H.H. Loosli, B.E. Lehmann, R. Purtschert, A. Love, L. Sampson, D. Anthony, D. Cole, B. Davids, D.J. Morrissey, B.M. Sherrill, M. Steiner, R.C. Pardo, M. Paul, ^{81}Kr in the Great Artesian Basin, Australia: a new method for dating very old groundwater, Earth and Planetary Science Letters 182 (2000) 103–113.

[119] B. Levin, H. Kromer, M. Schoch-Fischer, M. Bruns, D. Münnich, J.C. Berdau, K.O. Vogel, Münnich, 25 years of tropospheric ^{14}C observations in central Europe, Radiocarbon 27 (1) (1985) 1–19.

[120] H.A.J. Meijer, M.H. Pertuisot, J. van der Plicht, High-accuracy ^{14}C measurements for atmospheric CO_2 samples by AMS, Radiocarbon 48 (3) (2006) 355–372.

[121] C. Bronk Ramsey, C.A.M. Brenninkmeijer, P. Jöckel, H. Kjeldsen, J. Masarik, Direct measurement of the radiocarbon production at altitude, Nuclear Instruments and Methods B 259 (2007) 558–564.

[122] C.A.M. Brenninkmeijer, M.R. Manning, D.C. Lowe, G. Wallace, R.J. Sparks, A. Volz-Thomas, Interhemispheric asymmetry in OH abundance inferred from measurements of atmospheric ^{14}CO, Nature 356 (1992) 50–52.

[123] W. Rom, C.A.M. Brenninkmeijer, M. Bräunlich, R. Golser, M. Mandl, A. Kaiser, W. Kutschera, A. Priller, S. Puchegger, T. Röckmann, P. Steier, A detailed 2-year record of atmospheric ^{14}CO in the temperate northern hemisphere, Nuclear Instruments and Methods in Physics Research B 161–163 (2000) 780–785.

[124] V. Gros, M. Bräunlich, T. Röckmann, P. Jöckel, P. Bergamaschi, C.A.M. Brenninkmeijer, W. Rom, W. Kutschera, A. Kaiser, H.E. Scheel, M. Mandl, J. van der Plicht, G. Possnert, Detailed analysis of the isotopic composition of CO and characterization of he air masses arriving at Mount Sonnblick (Austrian Alps), Journal of Geophysical Research 106 (D3) (2001) 3179–3193.

[125] J. Lelieveld, C.A.M. Brenninkmeijer, P. Jö ckel, I.S.A. Isaksen, M.C. Krol, J.E. Mak, E. Dlugokencky, S.A. Montzka, P.C. Novelli, W. Peters, P.P. Tans, New directions: watching over tropospheric hydroxyl, Atmospheric Environment 40 (2006) 5741–5743.

[126] T.E. Graedel, P.J. Crutzen, Chemie der Atmosphäre, Spektrum Akademischer Verlag, Heidelberg, 1994, pp. 511.

[127] J.H. Butler, The NOAA Annual Greenhouse Gas Index (AGGI), updates are available on the web, <http://www.esrl.noaa.gov/gmd/aggi/>.

[128] D.C. Lowe, C.A.M. Brenninkmeijer, M.R. Manning, R. Sparks, G. Wallace, Radiocarbon determination of atmospheric methane at Baring Head, New Zealand, Nature 332 (1988) 522–525.

[129] R. Eisma, K. van der Borg, A.F.M. de Jong, W.M. Kieskamp, A.C. Veltkamp, Measurements of the ^{14}C content of atmospheric methane in The Netherlands to determine the regional emissions of $^{14}CH_4$, Nuclear Instruments and Methods in Physics Research B 92 (1994) 410–412.

[130] P. Quay, J. Stutsman, D. Wilbur, A. Snover, E. Dlugokencky, T. Brown, The isotopic composition of atmospheric methane, Global Biogeochemical Cycles 13 (1999) 445–461.

[131] V.V. Petrenko, A.M. Smith, E.J. Brook, D. Lowe, K. Riedel, G. Brailsford, Q. Hua, H. Schaefer, N. Reeh, R.F. Weiss, D. Etheridge, J.P. Severinghaus, $^{14}CH_4$ measurements in Greenland ice: investigating last glacial termination CH_4 sources, Science 324 (2009) 506–508.

[132] A. Priller, M. Berger, H.W. Gäggeler, E. Gerasopoulos, P.W. Kubik, C. Schnabel, L. Tobler, E.M. Wild, P. Zanis, C. Zerefos, Accelerator mass spectrometry of particle-bound ^{10}Be, Nuclear Instruments and Methods in Physics Research B 223–224 (2004) 601–607.

[133] M. Auer, D. Wagenbach, E.M. Wild, A. Wallner, A. Priller, H. Miller, C. Schlosser, W. Kutschera, Cosmogenic ^{26}Al in the atmosphere and the prospect of a ^{26}Al/^{10}Be chronometer to date old ice, Earth and Planetary Science Letters 287 (2009) 453–462.

[134] C. Bronk Ramsey, M.W. Dee, J.M. Rowland, T.F.G. Higham, S.A. Harris, F. Brock, A. Quiles, E.M. Wild, E.S. Marcus, A.J. Shortland, Radiocarbon-based chronology for dynastic Egypt, Science 328 (2010) 1554–1557.

[135] W. Kutschera, M. Bietak, E.M. Wild, C. Bronk Ramsey, M. Dee, R. Golser, K. Kopetzky, P. Stadler, P. Steier, U. Thanheiser, F. Weninger, The chronology of Tell el-Daba: a crucial meeting point of ^{14}C dating, archaeology, and Egyptology in the 2nd millennium BC, Radiocarbon 54 (3–4) (2012) 407–422.

[136] S.W. Manning, C. Bronk Ramsey, W. Kutschera, T. Higham, B. Kromer, P. Steier, E.M. Wild, Chronology for the Aegean LateBronze Age 1700–1400 B.C, Science 312 (2006) 565–569.

[137] W.L. Friedrich, B. Kromer, M. Friedrich, J. Heinemeier, T. Pfeiffer, S. Talamo, Santorini eruption radiocarbon dated to 1627–1600 B.C., Science 312 (2006) 548.

[138] E. Boaretto, Dating material in good archaeological contexts: the next challenge for radiocarbon, Radiocarbon 51 (1) (2009) 275–282.

[139] E.M. Wild, M. Teschler-Nicola, W. Kutschera, P. Steier, E. Trinkaus, W. Wanek, Direct dating of Early Upper Palaeolithic human remains from Mladec, Nature 435 (2005) 332–335.

[140] J. Zilhao, S.J.M. Davis, C. Duarte, A.M.M. Soares, P. Steier, E. Wild, Pego do Diabo (Loures, Portugal): dating the emergence of anatomical modernity in westernmost Eurasia, PLoS ONE 5 (1) (2010) 1–22, e8880.

[141] P. Mellars, J.C. French, Tenfold population increase in western Europe at the Neandertal-to-modern human transition, Science 333 (2011) 623–627.

[142] R.E. Wood, C. Barroso-Ruíz, M. Caparrós, J.F. Jordá Pardo, B. Galván Santos, T.F.G. Higham, Radiocarbon dating casts doubt on the late chronology of the Middle to Upper Palaeolithic transition in southern Iberia, Proceedings of the National Academy of Sciences 110 (2013) 2781–2786.

[143] K.L. Spalding, R.D. Bhardwaj, B.A. Bucholz, H. Druid, J. Frisén, Retrospective birth dating of cells in humans, Cell 122 (2005) 133–143.

[144] T. Levin, B. Naegler, M. Kromer, R.J. Diehl, A.J. Francey, L.P. Gomez-Pelaez, D. Steele, R. Wagenbach, D.E. Weller, Worthy, Observations and modelling of the global distribution and long-term trend of atmospheric $^{14}CO_2$, Tellus 62B (2010) 26–46.

[145] O. Bergmann, J. Liebl, S. Bernard, K. Alkass, M.S.Y. Yeaung, P. Steier, W. Kutschera, L. Johnson, M. Landén, H. Druid, K.L. Spalding, J. Frisén, The age of olfactory bulb neurons in humans, Neuron 74 (2012) 634–639.

[146] J. Liebl, P. Steier, R. Golser, W. Kutschera, K. Mair, A. Priller, I. Vorderhaid, E.M. Wild, Carbon background and ionization yield of an AMS system during ^{14}C measurements of microgram-size graphite samples, Nuclear Instruments and Methods in Physics Research B 294 (2013) 335–339.

[147] J.P. Day, J. Barker, S.J. King, R.V. Miller, J. Templar, J.S. Lilley, P.V. Drumm, G.W.A. Newton, L.K. Fifield, J.O.H. Stone, G.L. Allan, J.A. Edwardson, P.B. Moore, I.N. Ferrier, N.D. Priest, D. Newton, R.J. Talbot, J.H. Brock, L. Sánchez, C.B. Dobson, R.F. Itzhaki, A. Radunovic, M.W.B. Bradbury, Biological chemistry of aluminium studied using ^{26}Al and accelerator mass spectrometry, Nuclear Instruments and Methods in Physics Research Section B 92 (1994) 463–468.

[148] R.R. Johnson, D. Berkovits, E. Boaretto, Z. Gelbart, S. Ghelberg, O. Meirav, M. Paul, J. Prior, V. Sossi, E. Venczel, Calcium resorption from bone in a human studied by ^{41}Ca tracing, Nuclear Instruments and Methods in Physics Research Section B 92 (1994) 483–488.

[149] S.P.H.T. Freeman, B. Beck, J.M. Bierman, M.W. Cafee, R.P. Heaney, L. Holloway, R. Marcus, J.R. Southon, J.S. Vogel, The study of skeletal calcium metabolism with ^{41}Ca and ^{45}Ca, Nuclear Instruments and Methods in Physics Research B 172 (2000) 930–933.

[150] E. Denk, D. Hillegonds, J. Vogel, A. Synal, C. Geppert, K. Wendt, K. Fattinger, C. Hennessy, M. Berglund, R.F. Hurrell, T. Walczyk, Labeling the human skeleton with ^{41}Ca to assess changes in bone calcium metabolism, Analytical and Bioanalytical Chemistry 386 (2006) 1587–1602.

[151] K.W. Turteltaub, J.S. Felton, B.L. Gledhill, J.S. Vogel, J.R. Southon, M.W. Caffee, R.C. Finkel, D.E. Nelson, I.D. Proctor, J.C. Davis, Accelerator mass spectrometry in biomedical dosimetry: relationship between low-level exposure and covalent binding of heterocyclic amine carcinogens to DNA, Proceedings of the National Academy of Sciences 87 (1990) 5288–5292.

[152] G. Lappin, C.R. Garner, Big physics, small doses: the use of AMS and PET in human microdosing of development drugs, Nature Reviews 2 (2003) 233–240.

[153] C.R. Garner, Practical experience of using human microdosing with AMS analysis to obtain early human drug metabolism and PK, Bioanalysis 2 (2010) 429–440.

[154] W.S. Broecker, T. Peng, Z. Beng, Tracers in the Sea, Eldigio Press, Palisades, New York, 1982, pp. 690.

[155] W.S. Broecker, A. Mix, M. Andree, H. Oeschger, Radiocarbon measurements on coexisting benthic and planktic foraminifera shells: potential for reconstructing ocean ventilation times over the past 20000 years, Nuclear Instruments and Methods in Physics Research B 5 (1984) 331–339.

[156] W.S. Broecker, The great ocean conveyor, Oceanography 4 (1991) 79–89.

[157] W.S. Broecker, The carbon cycle and climate change: memoirs of my 60 years in science, Geochemical Perspectives 1 (2012) 221–339.

[158] S. Rahmstorf, Ocean circulation and climate during the past 120,000 years, Nature 419 (2002) 207–214.

[159] A.P. Mc Nichol, R.J. Schneider, K.F. von Reden, A.R. Gagnon, K.L. Elder, NOSAMS, R.M. Key, P.D. Quay, Ten years after—the WOCE AMS radiocarbon program, Nuclear Instruments and Methods in Physics Research Section B 172 (2000) 479–484.

[160] R.M. Key, A. Kozyr, C.L. Sabine, K. Lee, R. Wanninkhof, J.L. Bullister, R.A. Feely, F.J. Millero, C. Mordy, T.-H. Peng, A global ocean carbon climatology: results from Global Data Analysis Project (GLODAP), Global Biogeochemical Cycles 18 (2004) 1–23, GB4031.

[161] H.H. Loosli, Argon 39: a tool to investigate ocean water circulation and mixing, in: P.J. Fritz, Ch. Fontes (Eds.), Handbook of Environmental Isotope Geochemistry, vol. 3, Elsevier, Amsterdam, 1989, p. 387.

[162] P. Collon, M. Bichler, J. Caggiano, L. DeWayne Cecil, Y. El Masri, R. Golser, C.L. Jiang, A. Heinz, D. Henderson, W. Kutschera, B.E. Lehmann, P. Leleux, H.H. Loosli, R.C. Pardo, M. Paul, K.E. Rehm, P. Schlosser, R.H. Scott, W.M. Smethie Jr., R. Vondrasek, Development of an AMS method to study oceanic circulation characteristics using cosmogenic ^{39}Ar, Nuclear Instruments and Methods in Physics Research B 223–224 (2004) 428–434.

[163] P. Collon, M. Bowers, F. Calaprice, C. Galbiati, D. Henderson, T. Hohman, C.L. Jiang, W. Kutschera, H.Y. Lee, B. Loer, R.C. Pardo, M. Paul, E. Rehm, D. Robertson, C. Schmitt, R. Scott, R. Vondrasek, Reducing potassium contamination for AMS detection of ^{39}Ar with an electron-cyclotron-resonance ion source, Nuclear Instruments and Methods B 283 (2012) 77–83.

[164] J.-C. Gascard, G. Raisbeck, S. Sequeira, F. Yiou, K.A. Mork, The Norwegian Atlantic current in the Lofoten basin inferred from hydrological and tracer data (^{129}I) and its interaction with the Norwegian coastal current, Geophysical Research Letters 31 (2004) 1–5, L01308.

[165] L. Wacker, L.K. Fifield, S.G. Tims, Developments in AMS of ^{99}Tc, Nuclear Instruments and Methods in Physics Research B 223–224 (2004) 185–189.

[166] M.J. Keith-Roach, J.P. Day, L.K. Fifield, F.R. Livens, Measurement of ^{237}Np in environmental water samples by accelerator mass spectrometry, The Analyst 126 (2001) 58–61.

[167] S.R. Winkler, P. Steier, J. Carilli, Bomb fall-out ^{236}U as a global oceanic tracer using an annually resolved coral core, Earth and Planetary Letters 359–360 (2012) 124–130.

[168] E. Hodge, J. McDonald, M. Fischer, D. Redwood, Q. Hua, V. Levchenko, R. Drysdale, C. Waring, D. Fink, Using the ^{14}C bomb pulse to date young spaleothems, Radiocarbon 53 (2) (2011) 345–357.

[169] J.D.H. Wischusen, L.K. Fifield, R.G. Cresswell, Hydrology of Palm Valley, central Australia; a Pleistocene flora refuge? Journal of Hydrology 293 (2004) 20–46.

[170] J. Fabryka-Martin, H. Bentley, D. Elmore, P.L. Airey, Natural iodine-129 as an environmental tracer, Geochimica et Cosmochimica Acta 49 (1985) 337–347.

[171] A.J. Love, A.L. Herczeg, L. Sampson, R.G. Cresswell, L.K. Fifield, Sources of chloride and implications for ^{36}Cl dating of old groundwater, southwestern Great Artesian Basin, Water Resources Research 36 (6) (2000) 1561–1574.

[172] N.C. Sturchio, X. Du, R. Purtschert, B.E. Lehmann, M. Sultan, L.J. Patterson, Z.-T. Lu, P. Müller, T. Bigler, K. Bailey, T.P. O'Connor, L. You, One million year old groundwater in the Sahara revealed by krypton-81 and chlorine-36, Geophysical Research Letters 31 (2004) L5503.

[173] J. Welte, F. Ritterbusch, I. Steinke, M. Henrich, W. Aeschbach-Hertig, M.K. Oberthaler, Towards the realization of atom trap trace analysis for ^{39}Ar, New Journal of Physics 12 (2010) 1–14, 065031.

[174] W. Jiang, W. Williams, K. Bailey, A.M. Davis, S.-M. Hu, Z.-T. Lu, T.P. O'Connor, R. Purtschert, N.C. Sturchio, Y.R. Sun, P. Mueller, ^{39}Ar detection at the 10^{-16} isotopic abundance level with Atom Trap Trace Analysis, Physical Review Letters 106 (2011) 1–4, 103001.

[175] W. Jiang, K. Bailey, Z.-T. Lu, P. Mueller, T.P. O'Connor, C.-F. Cheng, S.-M. Hu, R. Purtschert, N.C. Sturchio, Y.R. Sun, W.D. Williams, G.-M. Yang, An atom counter for measuring ^{81}Kr and ^{85}Kr in environmental samples, Cosmochimica et Geochimica Acta 91 (2012) 1–6.

[176] N.A.A. Bertler, P.J. Barrett, Vanishing polar ice sheets, in: J. Dodson (Ed.), Changing Climates, Earth Systems and Society, International Year of Planet Earth, Springer, Dordrecht/Heidelberg/London/New York @Springer Science + Business Media B.V, 2010, pp. 49–83.

[177] M. Milankovitch, Kanon der Erdbestrahlungen und seine Anwendung auf das Eiszeitenproblem, Königl. Serb. Akad. Belgrad, 1941, p. 484 (New English Translation, 1998, Canon of Insolation and the Ice Age Problem. With Introduction and Biographical Essay by Nikola Pantic, Alven Global, 1998, ISBN 86-17-06619-9, pp. 636.

[178] Berger, The Milankovitch astronomical theory of paleoclimates: a modern view, in: A. Beer, K. Pounds, P. Beer (Eds.), Vistas in Astronomy, vol. 24, Pergamon Press, UK, 1960, pp. 103–122.

[179] A. Berger, M.F. Loutre, Insolation values for the climate of the last 10 million years, Quaternary Science Reviews 10 (1991) 297–317.

[180] W. Dansgaard, Stable isotopes in precipitation, Tellus 16 (1964) 436–468.

[181] W. Dansgaard, S.J. Johnsen, J. Møller, C.C. Langway Jr., One thousand centuries of climatic record from Camp Century on the Greenland Ice Sheet, Science 166 (1969) 377–380.

[182] EPICA Community Members, Eight glacial cycles from an Antarctic ice core, Nature 429 (2004) 623–628.

[183] C. Emiliani, Pleistocene temperatures, Journal of Geology 63 (1955) 538–578.

[184] N.J. Shackelton, Oxygen isotopes, ice volume and sea level, Quaternary Science Reviews 6 (1987) 183–190.

[185] M. Vonmoos, J. Beer, R. Muscheler, Large variations in Holocene solar activity: constraints from ^{10}Be in the Greenland Ice Core Project ice core, Journal of Geophysical Research 111 (2006) 1–14, A10105.

[186] F. Steinhilber, J.A. Abreu, J. Beer, Solar modulation during the Holocene, Astrophysics and Space Sciences Transactions 4 (2008) 1–6.

[187] D.E. Sugden, D.R. Marchant, N. Potter Jr., R.A. Souchez, G.H. Denton, C.C. Swisher III, J.-L. Tison, Preservation of Miocene glacier ice in East Antarctica, Nature 376 (1995) (1995) 412–414.

[188] J.M. Schäfer, H. Baur, G.H. Denton, S. Ivy-Ochs, D.R. Marchant, C. Schlüchter, R. Wieler, The oldest ice on Earth in Beacon Valley, Antarctica: new evidence from surface exposure dating, Earth and Planetary Science Letters 179 (2000) 91–99.

[189] H. Craig, T.E. Cerling, R.D. Willis, W.A. Davis, C. Joyner, N. Thonnard, Krypton 81 in Antarctic ice: first measurement of a krypton age in ancient ice, EOS, Transactions American Geophysical Union 71 (1990) 1825.

[190] J.M. Schaefer, G.H. Denton, M. Kaplan, A. Putnam, R.C. Finkel, D.J.A. Barrell, B.G. Andersen, R. Schwartz, A. Mackintosh, T. Chinn, C. Schlüchter, High-frequency Holocene glacier fluctuations in New Zealand differ from the northern signature, Science 324 (2009) 622–625.

[191] S. Ivy-Ochs, H. Kerschner, M. Maisch, M. Christl, P.W. Kubik, C. Schlüchter, Latest Pleistocene and Holocene glacier variations in the European Alps, Quaternary Science Reviews 28 (2009) 2137–2149.

[192] B.M. Goehring, J.M. Schaefer, C. Schluechter, N.A. Lifton, R.C. Finkel, A.J. Timothy Jull, N. Akçar, R.B. Alley, The Rhone Glacier was smaller than today for most of the Holocene, Geology 39 (2011) 679–682.

[193] K. Nicolussi, G.G. Patzelt, Discovery of early Holocene wood and peat on the fore field of the Pasterze Glacier, Eastern Alps, Austria, The Holocene 10 (2000) 191–199.

[194] T.M. Jenk, S. Szidat, D. Bolius, M. Sigl, H.W. Gäggeler, L. Wacker, M. Ruff, C. Barbante, C.F. Boutron, M. Schwikowski, A novel radiocarbon dating technique applied to an ice core from the Alps indicating late Pleistocene ages, Journal of Geophysical Research 114 (D14305) (2009) 1–8.

[195] U. Morgenstern, L.K. Fifield, S.G. Tims, R.G. Ditchburn, Progress in AMS measurement of natural ^{32}Si for glacier ice dating, Nuclear Instruments and Research in Physics Research B 268 (2010) 739–743.

[196] D. Lal, In situ produced cosmogenic isotopes in terrestrial rocks, Annual Review of Earth and Planetary Sciences 16 (1988) 355–388.

[197] D. Lal, Cosmic ray labeling of erosion surfaces: *in situ* nuclide production rates and erosion models, Earth and Planetary Science Letters 104 (1991) 424–439.

[198] J.C. Gosse, F.M. Phillips, Terrestrial in situ cosmogenic nuclides: theory and application, Quaternary Science Reviews 20 (2001) 1475–1560.

[199] D.W. Burbank, J. Leland, E. Fielding, R.S. Anderson, N. Brozovic, M.R. Reid, C. Duncan, Bedrock incision, rock uplift and threshold hillslopes in the northwestern Himalayas, Nature 379 (1996) 505–510.

[200] M. Lupker, P.-H. Blard, J. Lavé, C. France-Lanord, L. Leanni, N. Puchol, J. Charreau, D. Bourlès, ^{10}Be-derived Himalayan denudation rates and sediment budgets in the Ganga basin, Earth and Planetary Science Letters 333–334 (2012) 146–156.

[201] J.M. Schaefer, T. Faestermann, G.F. Herzog, K. Knie, G. Korschinek, J. Masarik, A. Meier, M. Poutivtsev, G. Rugel, C. Schlüchter, F. Serifiddin, G. Winckler, Terrestrial manganese-53—a new monitor of Earth surface processes, Earth and Planetary Science Letters 251 (2006) 334–345.

[202] T. Fujioka, L.K. Fifield, J.O. Stone, P.M. Vasconcelos, S.G. Tims, J. Chappell, In situ cosmogenic ^{53}Mn production rate from ancient low-denudation surface in tropic Brazil, Nuclear Instruments and Methods in Physics Research B 268 (2010) 1209–1213.

[203] W. Zhou, F. Xian, J.W. Beck, A.J.T. Jull, Z. An, Z. Wu, M. Liu, M. Chen, A. Priller, W. Kutschera, G.S. Burr, H. Yu, S. Song, P. Cheng, X. Kong, Reconstruction of 130-kyr relative geomagnetic intensities from ^{10}Be in two Chinese loess sections, Radiocarbon 52 (1) (2010) 129–147.

[204] D.E. Granger, P.F. Muzikar, Dating sediment burial with in situ-produced cosmogenic nuclides: theory, techniques, and limitations, Earth and Planetary Science Letters 188 (2001) 269–281.

[205] E. Boaretto, D. Berkovits, M. Hass, S.K. Hui, A. Kaufman, M. Paul, S. Weiner, Dating of prehistoric caves sediments and flints using ^{10}Be and ^{26}Al in quartz from Tabun Cave (Israel): progress report, Nuclear Instruments and Methods in Physics Research B 172 (2000) 767–771.

[206] G. Shen, X. Gao, B. Gao, D.E. Granger, Age of Zhoukoudian Homo erectus determined with ^{26}Al/^{10}Be burial dating, Nature 458 (2009) 198–200.

[207] J. Masarik, R.C. Reedy, Effects of bulk chemical composition on nuclide production processes in meteorites, Geochimica et Cosmochimica Acta 58 (1994) 5307–5317.

[208] R. Michel, Long-lived radionuclides as tracers in terrestrial and extraterrestrial matter, Radiochimica Acta 87 (1999) 47–73.

[209] K. Nishiizumi, D.E. Elmore, P.W. Kubik, Update on terrestrial ages of Antarctic meteorites, Earth and Planetary Letters 93 (1989) 299–313.

[210] J. Klein, D. Fink, R. Middleton, K. Nishiizumi, J. Arnold, Determination of the half-life of ^{41}Ca from measurements of Antarctic meteorites, Earth and Planetary Letters 103 (1991) 79–83.

[211] W. Kutschera, I. Ahmad, B.G. Glagola, R.C. Pardo, K.E. Rehm, D. Berkovits, M. Paul, J.R. Arnold, K. Nishiizumi, Accelerator mass spectrometry of ^{59}Ni in extraterrestrial matter, Nuclear Instruments and Methods B 73 (1993) 403–412.

[212] C. Schnabel, S. Xue, P. Ma, G.F. Herzog, K. Fifield, R.G. Cresswel, M.L. di Tada, P. Hausladen, R.C. Reedy, Nickel-59 in surface layers of lunar basalt 74275: implications for the solar alpha particle flux, Lunar Planetary Science XXXI (2000) 1778.

[213] K. Knie, G. Korschinek, T. Faestermann, C. Wallner, J. Scholten, W. Hillebrand, Indication for supernova produced ^{60}Fe activity on Earth, Physical Review Letters 83 (1999) 18–21.

[214] K. Knie, G. Korschinek, T. Faestermann, E.A. Dorfi, G. Rugel, A. Wallner, ^{60}Fe anomaly in a deep-sea manganese crust and implications for a nearby supernova source, Physical Review Letters 93 (2004) 1–4, 171103.

[215] C. Fitoussi, G.M. Raisbeck, K. Knie, G. Korschinek, T. Faestermann, S. Goriely, D. Lunney, M. Poutivtsev, G. Rugel, C. Waelbroeck, A. Wallner, Search for supernova-produced ^{60}Fe in a marine sediment, Physical Review Letters 101 (2008) 1–4, 121101.

[216] S. Bishop, R. Egli, Discovery prospects for a supernova signature of biogenic origin, Icarus 212 (2011) 960–962.

[217] E. Zinner, Stellar nucleosynthesis and the isotopic composition of presolar grains from primitive meteorites, Annual Review of Earth and Planetary Science 26 (1998) 147–188.

[218] A. Wallner, K. Melber, S. Merchel, U. Ott, O. Forstner, R. Golser, W. Kutschera, A. Priller, P. Steier, Stable platinum isotope measurements in presolar nanodiamonds by TEAMS, Nuclear Instruments and Methods in Physics Research B 294 (2013) 496–502.

[219] Q.R. Ahmad, et al., Direct evidence for neutrino flavor transformation from neutral–current interactions in the Sudbury Neutrino Observatory (SNO collaboration), Physical Review Letters 89 (2002) 1–6, 011301.

[220] W.C. Haxton, C.W. Johnson, Geochemical integrations of the neutrino flux from stellar collapses, Nature 333 (1988) 325–329.

[221] M.S. Freedman, C.M. Stevens, E.P. Horwitz, L.H. Fuchs, J.L. Lerner, L.S. Goodman, W.J. Childs, J. Hessler, Solar neutrinos: proposal for a new test, Science 193 (1976) 1117–1119.

[222] W. Henning, W. Kutschera, H. Ernst, G. Korschinek, P. Kubik, W. Mayer, H. Morinaga, E. Nolte, U. Ratzinger, M. Müller, D. Schüll, The ^{205}Tl experiment, in: M.L. Cherry, K. Lande, W.A. Fowler (Eds.), Solar Neutrinos and Neutrino Astronomy, 126, American Institute of Physics Conference Proceedings, 1985, pp. 203–211.

[223] W. Henning, D. Schüll, On isobar separation and accelerator mass spectrometry of ^{250}Pb, Nuclear Instruments and Methods in Physics Research A271 (1988) 324–327.

[224] M.K. Pavicevic, E.M. Wild, G. Amthauer, M. Berger, B. Boev, W. Kutschera, A. Priller, T. Prohaska, I. Steffan, AMS measurements of ^{26}Al in quartz to assess the cosmic ray background for the geochemical solar neutrino experiment LOREX, Nuclear Instruments and Methods in Physics Research B 223–224 (2004) 660–667.

[225] G.A. Cowan, W.C. Haxton, Solar neutrino production of technetium-97 and technetium-98, Science 216 (1982) 51–54.

[226] K. Wolfsberg, G.A. Cowan, E.A. Bryant, K.S. Daniels, S.W. Downey, W.C. Haxton, V.G. Niesen, N.S. Nogar, C.M. Miller, D.J. Rokop, The molybdenum solar neutrino experiment, in: M.L. Cherry, K. Lande, W.A. Fowler (Eds.), Solar Neutrinos and Neutrino Astronomy, 126, American Institute of Physics Conference Proceedings, 1985, pp. 196–202.

[227] G. Herrmann, Superheavy-element research, Nature 280 (1979) 543–549.

[228] G.N. Flerov, G.M. Ter-Akopian, Superheavy nuclei, Reports on Progress in Physics 46 (1983) 817–875.

[229] P. Armbruster, G. Münzenberg, An experimental paradigm opening the world of superheavy elements, The European Physical Journal H37 (2012) 237–309.

[230] W. Stephens, J. Klein, R. Zurmuhle, Search for naturally occurring superheavy element $Z = 110$, $A = 294$, Physical Review C 21 (1980) 1664–1666.

[231] D.N. Schramm, W.A. Fowler, Synthesis of superheavy elements in the r-process, Nature 231 (1971) 103–106.

[232] A. Marinov, I. Rodushkin, Y. Kashiv, L. Halicz, I. Segal, A. Pape, R.V. Gentry, H.W. Miller, D. Kolb, R. Brandt, Existence of long-lived isomeric states in naturally occurring neutron-deficient Th isotopes, Physical Review C 76 (2007), 021303(R).

[233] A. Marinov, I. Rodushkin, A. Pape, Y. Kashiv, D. Kolb, R. Brandt, R.V. Gentry, H.W. Miller, L. Halicz, I. Segal, Existence of long-lived isotopes of a superheavy element in natural Au, International Journal of Modern Physics E 18 (2009) 621–629.

[234] A. Marinov, I. Rodushkin, D. Kolb, A. Pape, Y. Kashiv, R. Brandt, R.V. Gentry, H.W. Miller, Evidence for the possible existence of a long-lived superheavy nucleus with atomic mass number $A = 292$ and atomic number $Z \sim 122$ in natural Th, International Journal of Modern Physics E 19 (2010) 131–140.

[235] J. Lachner, I. Dillmann, T. Faestermann, G. Korschinek, M. Poutivtsev, G. Rugel, Search for long-lived isomeric states in neutron-deficient thorium isotopes, Physical Review C 78 (2008) 064313 (1–3).

[236] P. Ludwig, T. Faestermann, G. Korschinek, G. Rugel, I. Dillmann, L. Fimiani, S. Bishop, P. Kumar, Physical Review C 85 (2012) 1–8, 024315.

[237] F. Dellinger, O. Forstner, R. Golser, W. Kutschera, A. Priller, P. Steier, A. Wallner, G. Winkler, Search for a superheavy nuclide with $A = 292$ and neutron-deficient thorium isotopes in natural thorianite, Nuclear Instruments and Methods in Physics Research B 268 (2010) 1287–1290.

[238] F. Dellinger, W. Kutschera, O. Forstner, R. Golser, A. Priller, P. Steier, A. Wallner, G. Winkler, Upper limits for the existence of long-lived isotopes of roentgenium in natural gold, Physical Review C 83 (2011), 015801(1–9).

[239] F. Dellinger, O. Forstner, R. Golser, A. Priller, P. Steier, A. Wallner, G. Winkler, W. Kutschera, Ultrasensitive search for long-lived superheavy nuclides in the mass range $A = 288$ to $A = 300$ in natural Pt, Pb, and Bi, Physical Review C 83 (2011) 1–14, 065806.

[240] M.A. Stoyer, Island ahoy!, Nature 442 (2006) 876–877.

[241] D. Elmore, N. Anantaraman, H.W. Fulbright, H.E. Gove, H.S. Hans, K. Nishiizumi, M.T. Murrell, M. Honda, Half-life of ^{32}Si from tandem-accelerator mass spectrometry, Physical Review Letters 45 (1980) 589–592.

[242] W. Kutschera, W. Henning, M. Paul, R.K. Smither, E.J. Stephenson, J.L. Yntema, D.E. Alburger, J.B. Cumming, G. Harbottle, Measurement of the ^{32}Si half-life via accelerator mass spectrometry, Physical Review Letters 45 (1980) 592–596.

[243] D. Frekers, W. Henning, W. Kutschera, K.E. Rehm, R.K. Smither, J.L. Yntema, R. Santo, B. Stievano, N. Trautmann, Half-life of ^{44}Ti, Physical Review C 28 (1983) 1756–1762.

[244] W. Kutschera, P.J. Billquist, D. Frekers, W. Henning, K.J. Jensen, X. Ma, R. Pardo, M. Paul, K.E. Rehm, R.K. Smither, J.L. Yntema, L.F. Mausner, Half-life of ^{60}Fe, Nuclear Instruments and Methods in Physics Research B 5 (1984) 430–435.

[245] European Fusion Development Agreement (EFDA), Fusion electricity: a roadmap to the realisation of fusion energy, 2012 http://www.efda.org/wpcms/wp-content/uploads/2013/01/JG12.356-web.pdf?91a98e

[246] M. Friedrich, W. Pilz, N. Bekris, M. Glugla, M. Kiisk, V. Liechtenstein, A small and compact AMS facility for tritium depth profiling, Nuclear Instruments and Methods in Physics Research B 223–224 (2004) 21–25.

[247] A. Wallner, S.V. Chuvaev, A.A. Filatenkov, Y. Ikeda, W. Kutschera, G. Mertens, A. Priller, W. Rochow, P. Steier, H. Vonach, Precise measurement of the ^{27}Al(n, 2n)^{26g}Al excitation function near threshold and its relevance for fusion-plasma technology, The European Physical Journal A 17 (2003) 285–296.

[248] G. Wallerstein, I. Iben Jr., P. Parker, A. Merchant Boesgaard, G.M. Hale, A.E. Champagne, C.A. Barnes, F. Käppeler, V.V. Smith, R.D. Hoffman, F.X. Timmes, C. Sneden, R.N. Boyd, B.S. Meyer, D.L. Lambert, Synthesis of the elements in stars: forty years of progress, Reviews of Modern Physics 69 (1997) 995–1084.

[249] A. Wallner, Nuclear astrophysics and AMS—probing nucleosynthesis in the lab, Nuclear Instruments and Methods in Physics Research B 268 (2010) 1277–1282.

[250] A. Wallner, M. Bichler, K. Buczak, D. Fink, O. Forstner, R. Golser, M.A.C. Hotchkis, A. Klix, A. Krasa, W. Kutschera, C. Lederer, A. Plompen, A. Priller, D. Schumann, V. Semkova, P. Steier, High-sensitivity isobar-free AMS measurements and reference materialsfor ^{55}Fe, ^{68}Ge and ^{202g}Pb, Nuclear Instruments and Methods in Physics Research B 294 (2013) 374–381.

[251] W. Ratynski, F. Käppeler, Neutron capture cross section of ^{197}Au: a standard for stellar nucleosynthesis, Physical Review C 37 (1988) 595–604.

[252] C. Wiesner, L.P. Chau, H. Dinter, M. Droba, M. Heilmann, N. Joshi, D. Mäder, A. Metz, O. Meusel, I. Müller, D. Noll, H. Podlech, U. Ratzinger, H. Reichau, R. Reifarth, A. Schempp, S. Schmidt, W. Schweizer, K. Volk, C. Wagner, Proton driver Linac for the Frankfurt neutron source, American Institute of Physics Conference Proceedings 1265 (2010) 487–492.

[253] D.L. Preston, Y. Shimizu, D.A. Pierce, A. Suyama, K. Mabuchi, Studies of mortality of atomic bomb survivors. Report 13: solid cancer and noncancer disease mortality: 1950–1997, Radiation Research 160 (2003) 381–407.

[254] W. Rühm, K. Kato, G. Korschinek, H. Morinaga, E. Nolte, ^{36}Cl and ^{41}Ca depth profiles in a Hiroshima granite stone and the dosimetrie system 1986, Zeitschrift für Physik A 341 (1992) 235–238.

[255] T. Huber, W. Rühm, K. Kato, S.D. Egbert, F. Kubo, V. Lazarev, E. Nolte, The Hiroshima thermal-neutron discrepancy for ^{36}Cl at large distances. Part I: new ^{36}Cl measurements in granite samples exposed to A-bomb neutrons, Radiation and Environmental Physics 44 (2005) 75–86.

[256] E. Nolte, T. Huber, W. Rühm, K. Kato, V. Lazarev, L. Schultz, The Hiroshima thermal-neutron discrepancy for ^{36}Cl at large distances. Part II: natural in situ production as a source, Radiation and Environmental Biophysics 44 (2005) 87–96.

[257] A. Wallner, W. Rühm, G. Rugel, N. Nakamura, A. Arazi, T. Faestermann, K. Knie, H.J. Maier, G. Korschinek, ^{41}Ca in tooth enamel. Part I: a biological signature of neutron exposure in atomic bomb survivors, Radiation Research 174 (2010) 137–145.

[258] W. Rühm, A. Wallner, H. Cullings, S.D. Egbert, N. El-Faramawy, T. Faestermann, D. Kaul, K. Knie, G. Korschinek, N. Nakamura, J. Roberts, G. Rugel, 41Ca in tooth enamel. Part II: a means for retrospective biological neutron dosimetry in atomic bomb survivors, Radiation Research 174 (2010) 146–154.

[259] T. Straume, G. Rugel, A.A. Marchetti, W. Rühm, G. Korschinek, J.E. McAninch, K. Carroll, S. Egbert, T. Faestermann, K. Knie, R. Martinelli, A. Wallner, C. Wallner, Measuring fast neutrons in Hiroshima at distances relevant to atomic-bomb survivors, Nature 424 (2003) 539–542.

[260] P. Lindahl, S.-H. Lee, P. Worsfold, M. Keith-Roach, Plutonium isotopes as tracers for ocean processes: a review, Marine Environmental Research 69 (2010) 73–84.

[261] E. Hrnecek, P. Steier, A. Wallner, Determination of plutonium in environmental samples by AMS and alpha spectrometry, Applied Radiation and Isotopes 63 (2005) 633–638.

[262] R. Eigl, M. Srncik, P. Steier, G. Wallner, ^{236}U/^{238}U and ^{240}Pu/^{239}Pu isotopic ratios in small (2 L) sea and river water samples, Journal of Environmental Radioactivity 116 (2013) 54–58.

[263] B.A. Buchholz, S.R. Biegalski, S.M. Whitney, S.J. Tumey, C.J. Weaver, Basis for developing samarium AMS for fuel cycle analysis, Nuclear Instruments and Methods in Physics Research B 268 (2010) 773–775.

[264] P. Andersson, A.O. Lindahl, D. Hanstorp, C.C. Havener, Y. Liu, Y. Liu, Nearly complete isobar suppression by photodetachment, Journal of Applied Physics 107 (2010) 1–3, 026102.

[265] A.E. Litherland, I. Tomski, X.-L. Zhao, L.M. Cousins, J.P. Doupé, G. Javahery, W.E. Kieser, Isobar separation at very low energy for AMS, Nuclear Instruments and Methods in Physics Research B 259 (2007) 230–235.

[266] M. Salehpour, K. Hakansson, G. Possnert, Accelerator mass spectrometry of ultra-small samples with applications in the biosciences, Nuclear Instruments and Methods in Physics Research B 294 (2013) 97–103.

[267] L. Wacker, S.M. Fahrni, I. Hajdas, M. Molnar, H.-A. Synal, S. Szidat, Y.L. Zhang, Versatile gas interface for routine radiocarbon analysis with a gas ion source, Nuclear Instruments and Methods in Physics Research B 294 (2013) 315–319.

[268] M.L. Roberts, K.F. von Reden, J.R. Burton, C.P. McIntyre, S.R. Beaupré, A gas-accepting ion source for accelerator mass spectrometry: progress and applications, Nuclear Instruments and Methods in Physics Research B 294 (2013) 296–299.